EurJIC
European Journal of Inorganic Chemistry

A Journal of
ChemPubSoc Europe

Accepted Article

Title: Multidentate pyridyl-aminophosphinite and pyridyl-phosphoramidite ruthenium(II) complexes: Synthesis, structure and application as levulinic acid hydrogenation pre-catalysts

Authors: Greshon Amenuvor, Charles K Rono, James Darkwa, and Banothile C.E. Makhubela

To be cited as: *Eur. J. Inorg. Chem.* 10.1002/ejic.201900640

Link to VoR: http://dx.doi.org/10.1002/ejic.201900640

WILEY-VCH

WILEY-VCH

FULL PAPER

Multidentate pyridyl-aminophosphinite and pyridyl-phosphoramidite ruthenium(II) complexes: Synthesis, structure and application as levulinic acid hydrogenation pre-catalysts

Gershon Amenuvor, [a] Charles K. Rono,[a] James Darkwa*,[a] and Banothile C. E. Makhubela*[a]

Abstract: Novel multidentate pyridyl-aminophosphinite (**L1**) and pyridyl-phosphoramidite (**L2**) ligands of N^P^P^N-donor system have been synthesised *via* a series of simple steps. The ligands are symmetrical and as a result, their reactions with $[Ru(p\text{-cymene})Cl_2]_2$ and $[Ru(benzene)Cl_2]_2$ lead to the formation of four monodentate bimetallic complexes (**1-4**) that retain the symmetry of the ligands. *Meso* and *racemic* mixtures (*rac*) of bidentate bimetallic complexes **5-8** were formed from the monodentate complexes through coordination of the pyridine nitrogen atoms to the two metal centres. The isomerism occurs at each metal center, which was evidenced by $^{31}P\{^1H\}$, ^1H NMR spectroscopy and single crystal X-ray diffraction. The complexes were active towards hydrogenation of levulinic acid (LA) to γ-valerolactone (GVL) using formic acid as the hydrogen source. The complexes are active at relatively low temperatures and are able to perform the hydrogenation in the absence of any additional solvent apart from the reagents to give high TON of 3 600. The catalysts are recyclable up to the fourth cycle, following which 20% loss of activity is seen.

Introduction

The design of multidentate ligands containing mixed-donor atoms to functionalise transition metal centres is a subject of growing interest in coordination and organometallic chemistry.[1-3] Multidentate mixed-donor ligands function cooperatively in stabilizing metal centres due to their different binding abilities and bridging effect between two or more metal centres.[4] These synergistic effects are helpful in making complexes containing multidentate mixed-donor ligands very attractive for several applications including catalysis.[5-7] Catalytic activity of these ligands also results from easy dissociation of the weakly coordinated donor atoms to create vacant site for the incoming substrate. These ligand types are generally large in structure and therefore form robust complexes with stable kinetic and thermodynamic properties as compared to monodentate ligands.[8] Due to their chelating ability, these ligands' conformational mobility is controlled effectively by choosing a suitable bridging or linker size.[1]

In general, multidentate mixed-donor ligands that have been reported comprise of phosphorus, nitrogen, sulphur and oxygen donor atoms in different binding arrangements such as P^N^S and P^N^N^P systems.[9-11] An example of the latter is the iminophosphorane-phosphine reported by Le Floch and co-workers.[12-13] Both iron(II) and rhodium(III) complexes of this ligand have been found to be very effective in catalysing transfer hydrogenation of acetophenone and its derivatives to the respective alcohols. A year later, Sabo-Etienne and co-workers found that a ruthenium(II) complex bearing the iminophosphorane-phosphine ligand was very effective in the hydrogenation of both aromatic and aliphatic ketones.[14] Worthy of attention is the extremely efficient trans-$[RuCl_2((S,S)\text{-}cyP_2(NH)_2]$ complex of P^N^N^P systems used for transfer hydrogenation of aromatic ketones reported by Noyori and co-workers.[15]

Tetradentate N^P^P^N type of mix-donor ligands are also promising candidates for designing reactive transition metal catalysts. In particular, very few examples of these ligands that can coordinate to two metal centres through all four donor atoms are known.[4,16-17] One such ligand system is the 2-$PyCH_2(Ph)P(CH_2)_nP(Ph)CH_2$-2-Py (Py = pyridine, n = 2-4) (Figure 1 (**a**)) reported by Nakajima and co-workers, that bound to two metal centres in a bidentate fashion providing a good platform for homo- and hetero-dinuclear systems. The N^P^P^N system (Figure 1(**b**)) reported by Mezzetti and co-workers forms a very stable complex with iron(II) compared to P^N^N^P system due to the hard N-donors (and its less bulkiness) at the terminals which matches with the hard metal centre.[17]

Our group has reported application of P^N pyrazolyl-phosphite ruthenium(II) and pyrazolyl-phosphinite ruthenium(II) complexes for LA hydrogenation and noticed the catalysts are effective and selective for GVL formation using molecular hydrogen.[18] By

[a] Dr G. Amenuvor, Mr C.K. Rono, Prof J Darkwa,
Dr B C. E. Makhubela
Chemistry Department
University of Johannesburg
Auckland Park Campus, 2006, South Africa
E-mail: bmakhubela@uj.ac.za

Supporting information for this article is given via a link at the end of the document.

carefully selecting phosphinocarboxylate ligands, we were able to design another heterometallic Ru^Zn-based catalyst system.[19a] This system outperformed the pyrazolyl-phosphite ruthenium(II) and pyrazolyl-phosphinite ruthenium(II) system in LA hydrogenation when formic acid was used as the hydrogen source. LA is a product form cellulosic biomass hydrolysis → dehydration → rehydration and has been identified as as one of the top 12 building block chemicals.[19b] Hydrogenation of LA leads to the formation of γ-valerolactone (GVL) which is useful as a bio-solvent, fuel additive and an illuminating liquid fuel.[19c-d]

Of interest to us in this work are the pyridyl-phosphoramidite and pyridyl-aminophosphinite P^N^N^P systems (which are less explored in catalyst design) to stabilize two ruthenium metal centres, forming a homonuclear bimetallic system. Having nitrogen bonded directly to phosphorus might place the electronic properties of these ligand systems between the traditional phosphines and the phosphinites or phosphites. The *π*-acceptor strength of the phosphorus in the pyridyl-phosphoramidite would be lessened compared to the phosphite analogues, for instance, the pyrazolyl-phosphite and pyrazolyl-phosphite systems.[20] With this modification, the properties and structures of their metal complexes would differ from those of the phosphines and phosphites analogues. It is envisaged that combination of the weak *π*-acceptor phosphorus due to P-N bond and weak σ-donor from the pyridine nitrogen could influence the catalytic activity of the complexes containing these ligands.

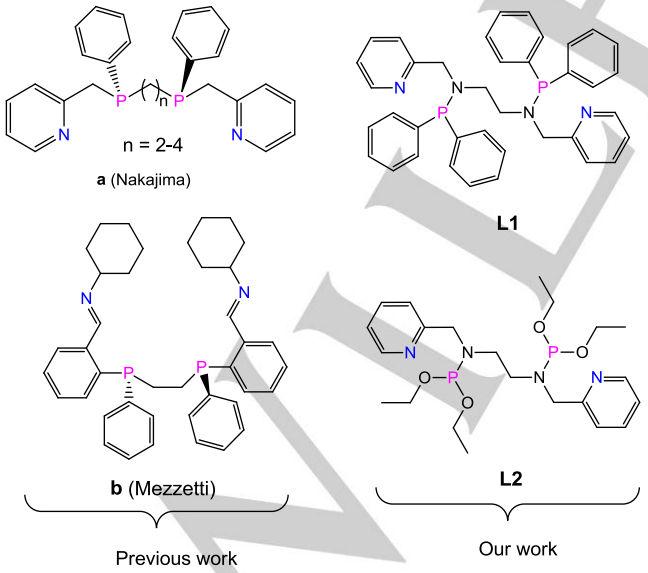

Figure 1. Example of N^P^P^N ligands previously reported and new ones prepared by us.

The uniqueness of these ligand systems is their variable coordination modes, which can allow them to tolerate coordination to two metal centres in either a mono- or bidentate-fashion depending on reaction conditions. Single coordination compounds with multiple metal ion sites can provide a unique set of properties that may enhance their activity in catalytic reactions.[21] We report herein the synthesis and characterization of pyridyl-aminophosphinite (**L1**) and pyridyl-phosphoramidite (**L2**) N^P^P^N ligands and their bimetallic ruthenium(II) complexes bearing benzene and *p*-cymene auxiliary ligands, and studies of the catalytic activities of the resulting complexes in hydrogenation of LA to GVL.

Results and Discussion

Synthesis of ligands L1 and L2

The synthesis of *N*^{1},*N*^{2}-bis(pyridin-2-ylmethylene)ethane-1,2-diamine (**C1**) was reported previously by several independent authors. Oshima and co-workers[22] reported the synthesis of this compound by refluxing 2-pyridylcarboxaldehyde and 1,2-ethylenediamine in ethanol for 1 h and obtained the product in 36% yield. El-Qisairi *et al*. also reported the synthesis of this compound in a similar manner to obtain 48% yield but at a longer reaction time of 24 h.[23] Other attempts to synthesise **C1** also lead to low yields.[24] We synthesised **C1** under solvent-free condition, where a mixture of the two reagents was stirred at 50 °C for 1 h to obtain over 99% yield without any work up. Reduction of the diimine was carried out in methanol at reflux for 2 h, as reported in literature[25] using sodium borohydride to afford *N*^{1},*N*^{2}-bis(pyridin-2-ylmethyl)ethane-1,2-diamine (**C2**) in 98% yield. The bis(pyridyl-aminophosphinite) and bis(pyridyl-phosphoramidite) ligands (**L1** and **L2**) were synthesised as shown in Scheme 1 by reacting **C2** with two equivalents of chlorodiphenylphosphine and diethyl chlorophosphite to obtain **L1** and **L2** respectively. Compound **L1** was obtained as a pale-yellow solid in 61% yield whereas **L2** was obtained as a pale-yellow viscous oil (83% yield) at room temperature. The ligands were characterised using ^{1}H, ^{31}P{^{1}H} and ^{13}C{^{1}H} NMR spectroscopy. Both ligands show an upfield shift in their ^{31}P{^{1}H} spectra with respect to the signals of the original phosphine and phosphite reagents.

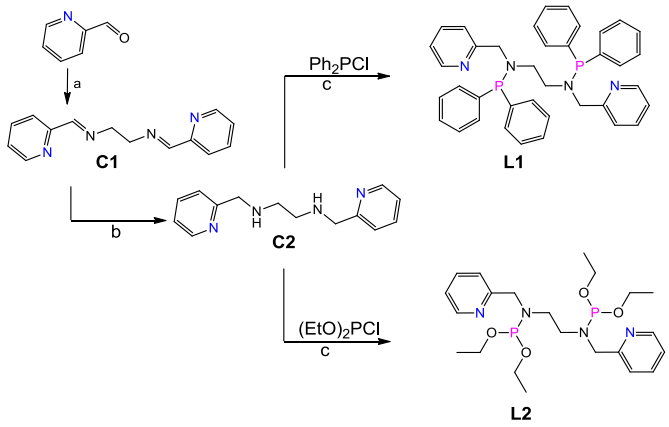

a) $CH_2NH_2CH_2NH_2$, 50 °C, 1 h; b) $NaBH_4$, EtOH, 80 °C, 2 h;
c) Et_3N, Diethyl ether, 0-5 °C, 3 h /12 h.

Scheme 1. Synthesis of bis(pyridyl-aminophosphinite) (**L1**) and bis(pyridyl-phosphoramidite) (**L2**) ligands**.**

The $^{31}P\{^1H\}$ signal of **L1** was observed as a single peak at 64.9 ppm, suggesting the symmetrical nature of the ligand. Similarly, a single major peak at 145.2 ppm in the $^{31}P\{^1H\}$ NMR spectrum of **L2** was observed. The symmetrical nature of the ligands supports Balakrishna and co-workers' findings on similar diphosphine system that contains a benzyl pendant in place of the pyridyl moiety.[26] However, the N^P^P^N system reported by Nakajima and co-workers have been found to exist as configurational isomers due the stereogenic phosphorus centres.[4] Formation of **L1** and **L2** was further confirmed by $^{13}C\{^1H\}$ NMR spectroscopy. In the $^{13}C\{^1H\}$ NMR spectra of the ligands, $^3J_{CP}$ and $^2J_{CP}$ couplings between the phosphorus and the ethylene carbons were observed. The coupling was observed for the methylene and 3° carbons of the pyridine as well (Figure S3).

Synthesis and characterisation of complexes

Synthesis of the neutral complexes was accomplished as shown in Scheme 2 by reacting ligands **L1** and **L2** with one molar equivalent of the metal precursors $[Ru(p\text{-cymene})Cl_2]_2$ and $[Ru(benzene)Cl_2]_2$ in dichloromethane at room temperature to afford monodentate bimetallic complexes **1-4**. The ligand coordination to the metal centre through the phosphorus atom is a fast reaction that occurs in 1 to 2 h with no sign of coordination of the pyridyl nitrogen as evidenced by changes observed in the $^{31}P\{^1H\}$ chemical shift. This sometimes requires a halide abstracting agent.[27] The complexes have been characterised by several characterisation techniques such as a combination of ^1H, $^{31}P\{^1H\}$ and $^{13}C\{^1H\}$ NMR spectra, high resolution mass spectrometry (HR-MS), infrared (IR) spectroscopy and elemental analysis. The $^{31}P\{^1H\}$ NMR spectroscopy suggests that the two phosphorus centres in the neutral bimetallic complexes are magnetically equivalent. This is indicated by the appearance of a single singlet in the $^{31}P\{^1H\}$ spectra of the complexes. There was a considerable downfield shift in the $^{31}P\{^1H\}$ NMR spectra of complexes **1** and **2**. Complexes **3** and **4** experienced an upfield shift of about 24 ppm in their $^{31}P\{^1H\}$ spectra compared to the free ligand. This is possibly due to the electron withdrawing ability of the ethoxy moieties on the phosphorus atom, which might increase the *π*-acceptor ability of the phosphorus.

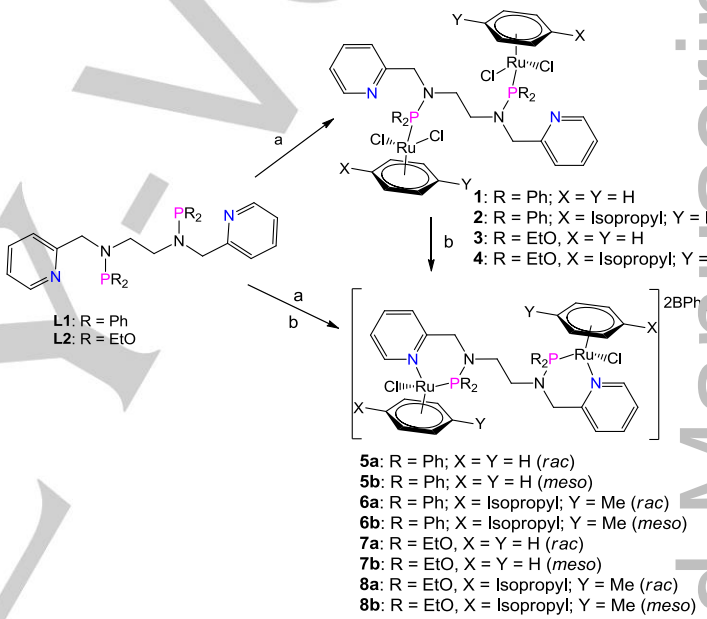

a) $[Ru(p\text{-cymene})Cl_2]_2$, DCM, r.t., 3 h; b) $2NaBPh_4$, DCM, MeOH, r.t., 16 h.

Scheme 2. Synthesis of mono- and bidentate bimetallic ruthenium(II) complexes **1-8**.

Further characterisation of the complexes with positive mode electrospray ionization high resolution mass spectrometry, HR-MS (ESI^+), revealed that the complexes were both singly and doubly (most stable fragments) charged in the mass spectrum (e.g. Figure S9). The bidentate complexes were formed as shown in Scheme 2, by treating the neutral complexes with two equivalents of sodium tetraphenylborate ($NaBPh_4$). Alternatively, *in situ* generation of the neutral complexes in dichloromethane followed by addition of two equivalents of $NaBPh_4$ in 4 mL of methanol at room temperature resulted in the formation of the cationic complexes **5**-**8** in good yields. The bidentate coordination of the ligands to the metal centres was established using several techniques including ^1H, $^{31}P\{^1H\}$ and $^{13}C\{^1H\}$ NMR spectroscopy

and single X-ray diffraction. Interestingly, two configurational isomers (*rac* and *meso* compounds) were obtained from each neutral complex upon coordination of the pyridyl nitrogen to the ruthenium centres. The *rac* and *meso* compounds are present in 1:1 ratio as determined by $^{31}P\{^{1}H\}$ and ^{1}H NMR spectroscopy. Isomers **5a**, **5b**, **6a** and **6b** have distinct solubility properties, which make their separation possible *via* washing with appropriate solvent or recrystallization.

Significant changes in chemical shifts have been observed in the ^{1}H NMR spectra of the bimetallic complexes. Notably among these is the diastereotopicity of the methylene (CH_2) protons adjacent to the pyridyl group that split into an AB quartet (ABq) fashion.[28] HR-MS analysis in both positive and negative modes also confirmed the formation of the cationic complexes. The positive mode HR-MS analysis shows the doubly charged fragments as the prominent peaks of the cationic portions of the complexes.

Crystal structure determination by single crystal X-ray crystallography

The crystal structures of the complexes show the presence of two metal centres in which there is coordination between the phosphorus atoms and metal centres. Close inspections of the structure of **2** (Figure 2) revealed that the sp^3 nitrogen atoms of the complexes have lost their trigonal pyramidal geometry and approach a trigonal planar geometry. This is true for some substituted nitrogen containing compounds having P-N bonds.[26,29] The loss of pyramidality at the sp^3 nitrogen centre leads to an increase in bond angles around the nitrogen atoms. For instance, the bond angles around N3 in the structure of **2** are 125.0(5)˚, 119.9(5)˚ and 114.4(6)˚ for P(2)–N(3)–C(26), P(2)–N(3)–C(34) and C(26)–N(3)–C(34) respectively. The larger bond angles around the sp^3 nitrogen atom are those involving the phosphorus atom. This is due to the larger size of phosphorus compared to the size of carbon atom. The sum of the bond angels around N3 is 359.3˚, which is just 0.7˚ less than 360˚. This indicates that the N3 is slightly lying out of plane with its three bonding partners.

The structures obtained from X-ray spectroscopy reveals the configuration at the metal centres of the cationic complexes. In the structure of **7b** (Figure 4), for instance, there is coordination of the pyridine nitrogen atoms to the two metal centres *via* chloride exchange, resulting in the formation of six-membered heterocyclic rings that assume a distorted boat conformation. The metal centres assume a piano stool conformation as usual. With the distorted boat conformation of the six-membered heterocyclic rings the methylene hydrogens occupy equatorial and axial positions. The axial hydrogen (H6A) points away from the nearby pyridine and ethylene hydrogens (H4 and H7A). On the other hand, H6B is pointed in the direction of H4 and H7A resulting in close contact interaction with both H4 and H7A. The close contact space-coupling is confirmed by the short distances observed for H4···H6B and H6B···H7A (ca. 2.3 Å). The intramolecular close contact H···H distances found in **5a**, **7b** and **8b** are listed in **Table 1**. The distorted trigonal planar geometry of the sp^3 nitrogen atoms is observed also in the complexes (Figures 4 and 5). In complexes **7b** and **8b** the sum of the three bond angles around N2 are 358.8˚ and 354.8˚ respectively. Here, **7b** seems to slightly approach planarity at the sp^3 nitrogen centre compared to **8b**, which has *p*-cymene at the metal centres. In **5a**, however, the sp^3 nitrogen centre is completely planar, giving a sum of the angles around the nitrogen to be 360˚. There is no general trend in the planarity at the sp^3 nitrogen centre for all the complexes. However, the nitrogen centre becomes more planar with increasing P(1)–N(2)–C(6) bond angle for the complexes **5a**, **7b** and **8b**. Complex **5a** contains the largest P(1)–N(2)–C(6) bond angle of 120.7˚ followed by **7b** (113.4˚) and **8b** (113.2˚). This trend could be due to possible strain on the non-planar heterocyclic ring formed involving the P(1)–N(2)–C(6) bonds.

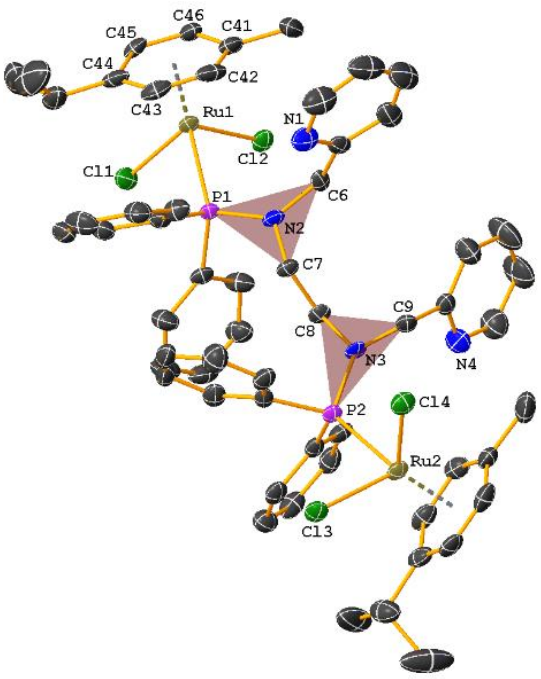

Figure 2. Structure of complex **2** in the crystal as determined by X-ray diffraction. Selected bond lengths (Å) and bond angles (°): Ru(1)–Cl(1), 2.404(2); Ru(1)–Cl(2), 2.415(2); Ru(1)–P(1), 2.359(2); Ru(1)–C(41), 2.211(9); Ru(1)–C(42), 2.187(8); Ru(1)–C(43), 2.184(9); Ru(1)–C(44), 2.242(8); Ru(1)–C(45), 2.232(8); Ru(1)–C(46), 2.231(8); P(1)–N(2), 1.668(6); N(2)–C(6), 1.452(10); N(2)–C(7), 1.481(9); P(1)–Ru(1)–Cl(1), 85.64(7); P(1)–Ru(1)–Cl(2), 91.34(8); Cl(1)–Ru(1)–Cl(2), 88.99(8); P(1)–N(2)–C(6), 125.0(5); P(1)–N(2)–C(7), 119.9(5); C(6)–N(2)–C(7), 114.4(6).

Table 1. Short H···H close contact distances determined in the crystal structures of the bimetallic complex.

Compound	5a	7b	8b
d(H4···H6B)	2.3 Å	2.3 Å	2.4 Å
d(H6B···H7A)	2.3 Å	2.3 Å	2.4 Å

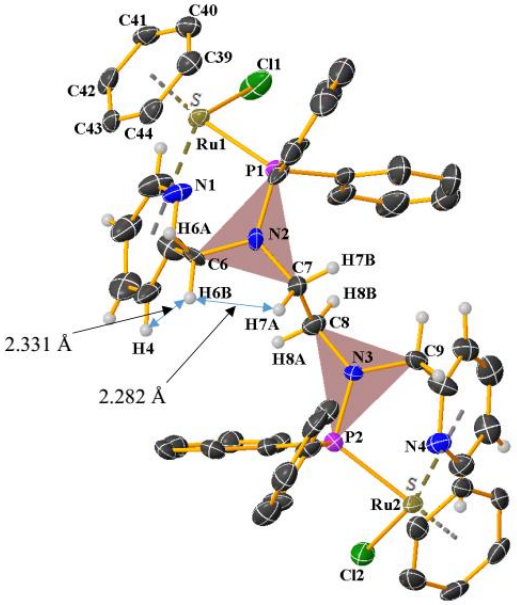

Figure 3. Structure of **5a** (*rac*) in the crystal as determined by X-ray diffraction. Some hydrogen atoms are omitted for clarity. Selected bond lengths (Å) and bond angles (°): Ru(1)–Cl(1), 2.388(4); Ru(1)–N(1), 2.110(12); Ru(1)–P(1), 2.310(4); Ru(1)–C(39), 2.223(14); Ru(1)–C(40), 2.200(13); Ru(1)–C(41), 2.248(12); Ru(1)–C(42), 2.256(12); Ru(1)–C(43), 2.205(12); Ru(1)–C(44), 2.196(14); P(1)–N(2), 1.666(10); N(2)–C(6), 1.475(15); N(2)–C(7), 1.499(14); P(1)–Ru(1)–Cl(1), 92.42(13); P(1)–Ru(1)–N(1), 87.3(3); N(1)–Ru(1)–Cl(1), 88.8(4); P(1)–N(2)–C(6), 120.7(8); P(1)–N(2)–C(7), 122.2(8); C(6)–N(2)–C(7), 117.1(9).

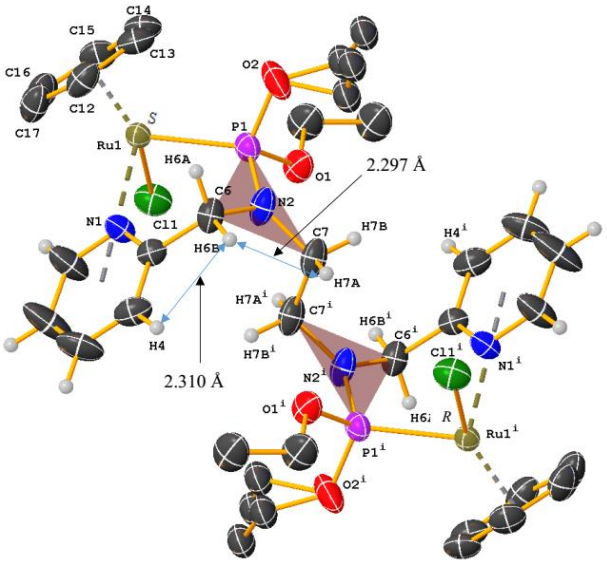

Figure 4. Structure of **7b** (*meso*) in the crystal as determined by X-ray diffraction. Some hydrogen atoms and counterions are omitted for clarity. Selected bond lengths (Å) and bond angles (°): Ru(1)–Cl(1), 2.3863(10); Ru(1)–N(1), 2.148(3); Ru(1)–P(1), 2.2629(10); Ru(1)–C(12), 2.189(4); Ru(1)–C(13), 2.185(4); Ru(1)–C(14), 2.210(4); Ru(1)–C(15), 2.194(4); Ru(1)–C(16), 2.264(4); Ru(1)–C(17), 2.267(4); P(1)–N(2), 1.636(3); N(2)–C(6), 1.470(5); N(2)–C(7), 1.476(5); P(1)–O(1), 1.582(3); P(1)–Ru(1)–Cl(1), 88.81(4); P(1)–Ru(1)–N(1), 89.33(9); N(1)–Ru(1)–Cl(1), 84.90(9); P(1)–N(2)–C(6), 114.4(2); P(1)–N(2)–C(7), 126.4(3); C(6)–N(2)–C(7), 118.0(3).

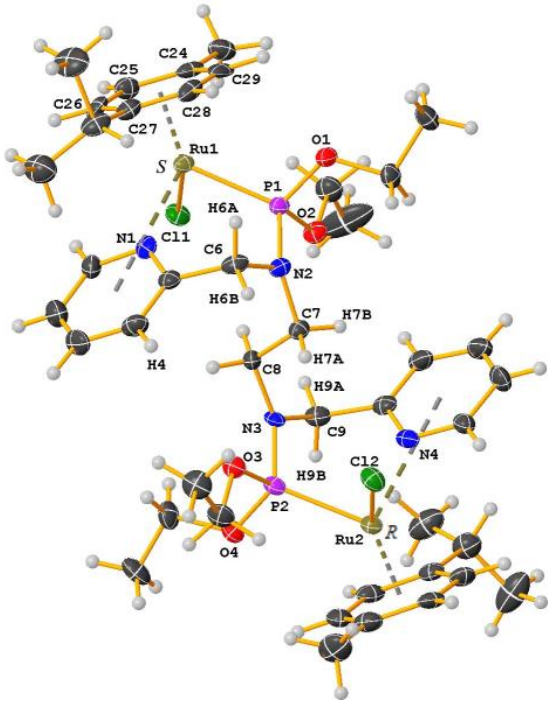

Figure 5. Structure of **8b** (*meso*)in the crystal as determined by X-ray diffraction. The counterions are omitted for clarity. Selected bond lengths (Å) and bond angles (°): Ru(1)–Cl(1), 2.3752(19); Ru(1)–N(1), 2.126(6); Ru(1)–P(1), 2.261(2); Ru(1)–C(24), 2.225(8); Ru(1)–C(25), 2.229(8); Ru(1)–C(26), 2.242(7); Ru(1)–

C(27), 2.251(8); Ru(1)–C(28), 2.205(8); Ru(1)–C(29), 2.203(7); P(1)–N(2), 1.648(7); N(2)–C(6), 1.471(10); N(2)–C(7), 1.475(9); P(1)–O(1), 1.594(5); P(1)–Ru(1)–Cl(1), 87.17(7); P(1)–Ru(1)–N(1), 88.34(18); N(1)–Ru(1)–Cl(1), 84.93(18); P(1)–N(2)–C(6), 113.2(5); P(1)–N(2)–C(7), 124.2(5); C(6)–N(2)–C(7), 117.4(6).

Hydrogenation of LA with formic acid

The hydrogenation reaction was initially performed using LA (10 mmol), FA (10 mmol), triethylamine (10 mmol) and 0.01 mmol (0.1 mol%) of pre-catalyst **1** at 120 °C. Triethylamine was chosen as the base for the reaction due to its effectiveness as reported previously. [19,30] The reactions involving **1** and the rest of the catalyst precursors were accompanied by CO_2 and H_2 generation as observed previously.[18-19,31] This was characterised by a rise in the pressure gauge reading and prolonged fizzing of the reaction mixture after opening the reactors. In a period of 12 h, 86% conversion of LA was obtained with 95% GVL selectivity and the rest being 4-hydroxyvaleric acid (4-HVA) (Table 2; entry 1). When the amount of the base was reduced to 50 mol% in attempts to optimize the reaction conditions, there was no significant change in LA conversion, neither did this affect selectivity of GVL. This indicates that the reaction does not require an equivalent amount of base for complete deprotonation of the formic acid to formate as the base is possibly regenerated when CO_2 and H_2 are formed from the formic acid decomposition (a possible mechanistic process that could be taking place concurrently with transfer mechanism). This is further supported by the presence of two upfield signals in the ^{1}H NMR spectrum of a mixture of isomers of **6a** and **6b** treated with formic acid at 120ºC for 30 minutes. (Figure S23). The the ^{1}H NMR spectrum shows two signals at -11.47 ppm and -14.43 ppm assigned to the Ru-H and the Ru-H_2 species respectively. The Ru-H is the catalytically active species and is formed at both ruthenium centres, within the bimetallic structure, and promotes the reaction simultaneoulsy. The reaction pathway is likely similar to what we previously proposed.[19a] This result together with our previous studies on LA hydrogenation show that the catalytic reactions are less dependent on the quantity of base used to initiate the reactions.[19a,32] With two molar equivalents of formic acid, there was an increase in the rate of the catalytic reaction, giving 94% LA conversion at the lower base concentration (50 mol%) and a shorter time of 8 h (Table 2; entry 3).

Table 2: Hydrogenation of LA using formic acid and **1-8**[a]

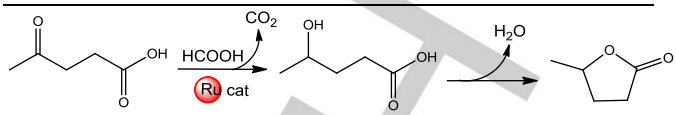

Entry	Cat. (mol %)	FA (equiv)	Et_3N (equiv)	Conversion (%)	GVL selectivity (%)[b]
1[c]	**1** (0.1)	1	1	86	95
2[c]	**1** (0.1)	1	0.5	85	96
3	**1** (0.1)	2	0.5	94	95
4	**2** (0.1)	2	0.5	90	93
5	**3** (0.1)	2	0.5	98	96
6	**4** (0.1)	2	0.5	98	93
7	**5a** (0.1)	2	0.5	89	94
8	**5b** (0.1)	2	0.5	87	91
9	**5** (0.1)	2	0.5	89	93
10	**6a** (0.1)	2	0.5	88	92
11	**6b** (0.1)	2	0.5	86	93
12	**6** (0.1)	2	0.5	89	92
13	**7** (0.1)	2	0.5	98	97
14	**8** (0.1)	2	0.5	100	97
15	**8** (0.1)	1	0.5	87	96

[a]**Conditions**: LA 10.0 mmol; 8 h; 120 °C; [b]The rest is 4-HVA; [c]12 h. Conversions were determined by ^{1}H NMR spectroscopy. Cat. 5, 6, 7 and 8 represent respective isomeric mixtures of **5a, 5b, 6a, 6b, 7a, 7b, 8a and 8b.**

The rest of the pre-catalysts (both those coordinted to the ligand in a monodentate and bidentate manner) were screened at these optimized conditions and the results are summarized in Table 2. All the pre-catalysts performed well, giving at least 90% conversions within 8 h. Among the neutral complexes, **3** and **4** which contain the phosphoramidite ligands performed better than their aminophosphinite analogues **1** and **2**. Both **3** and **4** gave 98% conversion while **1** and **2** gave 94% and 90% conversions respectively. Only traces of the intermediate 4-HVA were observed in all the reactions. The catalytic activities of the complexes **5**-**8** are very comparable with their monodentate analogues **1-4**. The isomers **5a**, **5b**, **8a** and **8b** demonstrate similar catalytic activity with conversions between 85% and 90%. This indicates that the configurations at the metal centres do not really influence the catalysts performance in terms of conversion. The isomeric mixtures of both **5** (**5a** and **5b**) and **8** (**8a** and **8b**) gave 89% conversion, which is slightly lower compared to the 94% and 90% obtained with their respective neutral counterparts **1** and **2**. This can be attributed to the extra stability associated with the chelating system, which might hinder ligand dissociation

from the metal centre for facile formation of the active species. Contrary to this, isomeric mixtures of **7** and **8** performed very similarly to their neutral counterparts **3** and **4**, giving 98% and 100% conversions respectively. With one molar equivalent of FA, the conversion with **8** decreased significantly to 87%, as observed with **1**. When comparing the current bimetallic catalysts with similar monometallic systems which we previously used for LA hydrogenation[18,19a], it becomes clear that there is merit to introducing two active sites in the catalyst structure. For example, monometallic phosphorus-donor (phosphinite and phosphite) ruthenium catalysts precurosor (at 0.1 mol% loading) showed 70% to 96 % conversion of LA in 16 hours[18], while similar catalysts precursors (**1**-**4**) coordinated in a monodentate fashion produced 93 % to 98 % conversion in half the time. Furthermore, the latter required more base additive (20 mmol) while inthis report we have established that lower base additive (5 mmol) is sufficient. The observation is further highlighted when the performance of monometallic cationic catalyst precursors, with P^N donor ligands, are compare to the current bimetallic systems (**5**-**8**). The former (at 0.1 mol % loading) displayed LA conversions in the range of 37 % to 68 % in 16 hours[18], while in this works the same loading of the pre-catalysts **5**-**8** gave conversions in the range of 87 % to 100 % in 8 hours.

In general, the pre-catalysts bearing phosphoramidite ligands (**3**, **4**, **7** and **8**) performed better than those bearing aminophosphinite ligands. This could be due to the electron withdrawing ability of the ethoxy moieties on the phosphorus. As a result, the metal centre becomes more electrophilic for the formate interaction prior to decomposition.

The effect of catalysts loading on the catalytic reaction was investigated using **8**. As mentioned previously, 100% conversion was obtained with pre-catalysts **8** at a catalyst loading of 0.1 mol%. Under similar conditions and with a lower catalyst loading of 0.05 mol%, the catalyst's performance was still very high; giving 90% conversion (Table 3; entry 1), which correspond to TON of 1 800. The conversion decreased drastically to 34% when the catalyst loading was reduced further to 0.025 mol%. However, higher conversion of 90% (3 600 TON) was observed with 0.025 mol% catalyst loading when the reaction time was prolonged to 24 h (Table 3; entry 4). The catalyst performance is comparable to most of the homogeneous metal catalysts reported for LA hydrogenation using formic acid as the hydrogen donor and under other similar conditions.[31,33] It is important to note that there are other homogeneous metal catalysts that have shown excellent activities in LA hydrogenation to GLV using molecular hydrogen.[44] The activity of the new bimetallic complexes is lower than that of the Ru^Zn hexa-heterometallic complexes we reported recently.[19]

To verify the homogeneity of the catalysts, mercury poisoning test was conducted using **4** and **8** as representatives of the neutral and cationic bimetallic catalyst precursors respectively. At similar conditions used previously in the presence of elemental mercury (0.02 mmol; 4 mg), the pre-catalysts (**4** and **8**) performed well to give 98% conversion each (Table 3; entries 5 and 6). This shows that the catalytic reactions involving the pre-catalysts happened with molecular complexes and no nanoparticles were involved regardless of the mode of ligand coordination to the metal centre.

Table 3: Catalyst loading investigation and homogeneity test

Entry	Cat. (mol %)	Conversion / %	GVL selectivity / %[b]	TON
1	**8** (0.05)	90	95	1800
2	**8** (0.025)	34	100	1360
3[c]	**8** (0.025)	66	100	2600
4[d]	**8** (0.025)	90	95	3600
5[e]	**4** (0.1)	98	95	980
6[e]	**8** (0.1)	99	93	990

[a]**Conditions**: LA 10.0 mmol; FA 10.0 mmol; Et_3N LA 5.0 mmol; 8 h; 120 °C; [b]The rest is 4-HVA; [c]140 °C; [d]24 h; [e]Hg 0.02 mmol (4.0 mg). Conversions were determined by ^1H NMR spectroscopy. Cat. **8** represents isomeric mixtures of **8a** and **8b.**

Time and temperature dependent studies

Time dependent study was carried out on pre-catalysts **7** and **8**. Of note is that the activity of the catalysts was very minimal (13% and 14% for **7** and **8** respectively) in the first hour of the reactions (Figure 6). A plausible reason could be that formation of the reactive catalyst species takes a relatively longer time to occur. The progress of the reactions, especially with **8**, became very rapid after the first one hour. The evidence of this is the high conversions obtained after the fourth hour into the reactions. Pre-catalyst **8** delivered the highest conversion of 92% in 4 h, after which the reaction proceeded gradually until the sixth hour where 99% was recorded. Pre-catalyst **7**, on the other hand, gave 67% conversion after 4 h and the reaction became faster between 4 h and 6 h compared to the performance of **8** within these hours.

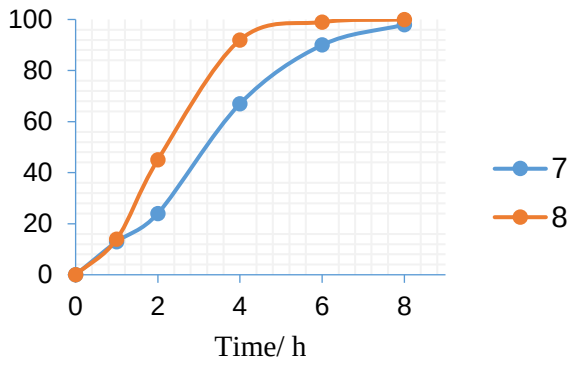

Figure 6. Time dependent study of LA hydrogenation with FA. LA 10 mmol; FA 20 mmol; catalyst precursor 0.01 mmol (0.1 mol%); Et_3N 5.0 mmol; 120 °C.

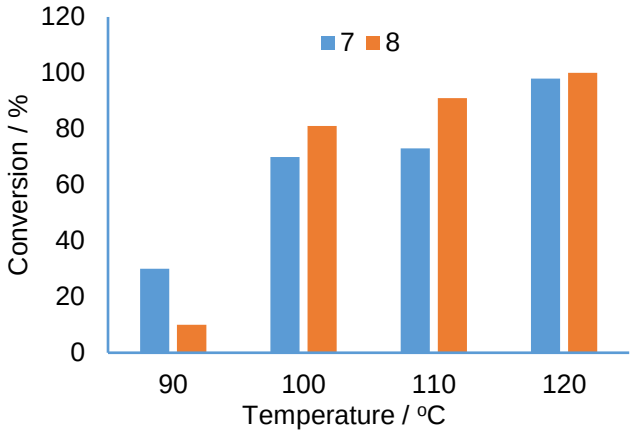

Figure 7. Temperature dependent study of LA hydrogenation with FA. LA 10 mmol; FA 20 mmol; catalyst precursor 0.01 mmol (0.1 mol%); Et_3N 5.0 mmol; 8 h.

Further studies on the behaviour of the catalysts show that temperature is very influential in their activity. As can be seen Figure 7, the catalysts respond greatly to temperature changes from 120 ºC down to 90 ºC. For catalyst **8**, a decrease in temperature by 10 ºC (from 120 to 110 ºC) resulted in decrease in LA conversion by 9%. Further reduction in temperature to 100 ºC lowered the LA conversion further by 9%. Unexpectedly, the activity of **8** became very poor giving only 10% conversion when the temperature was dropped to 90 ºC. In contrast, there was 30% conversion recorded with **7** at 90 ºC, which differs from **8** only by the *p*-cymene auxiliary ligands on the metals instead of benzene. The low activity of the catalysts at low temperature was accompanied by less amount of the mixture of CO_2 and H_2 gases generated during the reactions. The decomposition of the formate at the metal centre could be less favoured at low temperature. As a result, facile formation of the reactive catalytic species prior to the LA reduction is hindered by the coordinated formate. Another factor that could possibly play a role is solubility of hydrogen gas generated in the reaction mixture at low temperature. It has been reported that higher temperatures favour solubility of hydrogen gas in organic liquids.[35]

Effect of stirring on the catalytic reaction

Effect of stirring on the reaction kinetics has been studied using pre-catalyst **8** (0.1 mol%), 10 mmol of LA, 2 molar equivalents of FA, 0.5 molar equivalents of triethylamine at 120 ºC and 8 h reaction time. At low stirring speeds of 300 to 600 rpm, the LA conversion was constant at 90% (Figure S22). The reaction rate was enhanced at a higher stirring speed of 900 rpm, which resulted in 95% LA conversion. The low reaction rate at low stirring speed indicates that there is much resistance in mass transport at lower stirring speeds. This is due to high viscosity of the reaction mixture since the reactions were performed in the absence of any additional solvent apart from the reagents. At low stirring speeds, there is high resistance in the miscibility of the reaction mixture with the hydrogen gas generated. A slight increase of LA conversion (from 95 to 96%) was observed when the mixing speed was increased to 1200 rpm. Further increase in the stirring speed to 1500 rpm enhanced the reaction rate to give complete conversion at same 8 h. Reactions performed in gas-liquid[36-37] and viscous liquid-liquid[38-39] phases systems usually encounter resistance to miscibility and mass transport.

Catalysts recyclability

Stability of the catalysts was studied using **8** by performing recyclability experiments. The experiments were performed at the optimum temperature of 120 ºC, catalyst loading of 0.1 mol% and two molar equivalents of FA. The reactions were carried out for 6 h because 99% conversion was obtained with **8** after 6 h as shown in Figure 6. The first run resulted in 99% conversion after which GVL, water and triethylamine were removed from the reaction mixture *via* vacuum distillation at 80 to 85 ºC.[40] The

recovered catalyst was transferred into the reactor followed by addition of the appropriate amounts of LA, FA and triethylamine. This procedure was repeated four times. Data for the recycling experiment is summarized in Figure 8. The catalysts performance was maintained after the first cycle giving 99% conversion. However, its deactivation begun to occur gradually after the second cycle. This resulted in a slight decrease in conversion to 91% and 79% after the third and fourth cycles respectively.

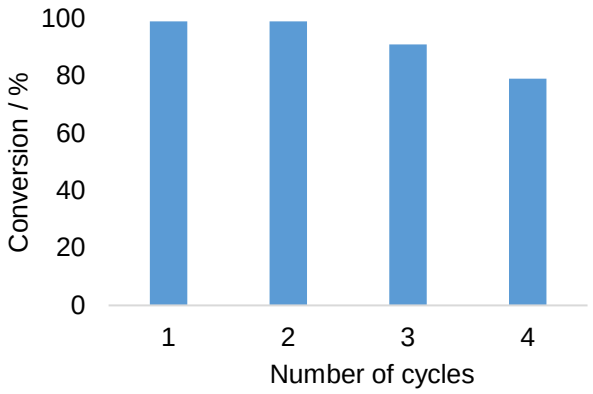

Figure 8. Catalyst recyclability study usin **8**: LA 10 mmol; FA 20 mmol; Catalyst **8** 0.01 mmol (0.1 mol%); Et_3N 5.0 mmol; 120 °C; 6 h. Conversions and selectivity were determined by ^1H NMR spectroscopy.

Conclusions

New multidentate ligands (**L1** and **L2**) of N^P^P^N-donor system that easily accommodate two metal centres leading to the formation of bimetallic complexes were synthesised and characterised. Reaction of the new ligands with $[Ru(p\text{-cymene})Cl_2]_2$ and $[Ru(benzene)Cl_2]_2$ lead to the formation of four neutral bimetallic complexes (**1-4**). *Meso* and *rac* cationic bimetallic complexes (**5-8**) were formed from the monodentate complexes through coordination of the pyridine nitrogen atoms to the two metal centres. The new complexes are catalytically active when screened for hydrogenation of LA to LA using formic acid as the hydrogen source and triethylamine as base. Low catalyst loadings of 0.025-0.1% resulted in over 90% selective conversion of LA to GVL. Doubling the amount of formic acid increases the catalytic conversion significantly while a decrease in the amount of base by half equivalent has no significant effect on the LA conversion. The complexes are active even at relatively low temperatures and can perform the hydrogenation in the absence of any additional solvent apart from the reagents. There is a loss of 20% of catalyst activity in the fourth cycle.

Experimental Section

Experimental Details.

All reactions were performed under a dry, deoxygenated nitrogen atmosphere using standard Schlenk techniques. All solvents were of analytical grade and were dried using MBRAUN SPS-800 solvent drying system and or distilled prior to use. Compounds 2-pyridinecarboxaldehyde (99%, Sigma-Aldrich), ethylenediamine (99.5%, Sigma-Aldrich), sodium borohydride (96%, Sigma-Aldrich), triethylamine (99%, Sigma-Aldrich), chlorodiphenylphosphine (98%, Sigma-Aldrich), diethyl chlorophosphite (96%, Aldrich), 1,4-cyclohexadiene(97%, Sigma-Aldrich), ruthenium(III) trichloride hydrate (99.98% trace metal basis, Sigma-Aldrich) dichloro(*p*-cymene)ruthenium(II) dimer (97%, Sigma-Aldrich), Levulinic acid (97%, Sigma-Aldrich) and formic acid (95%, Sigma-Aldrich) were of reagent grades and used as received. Dichloro(benzene)ruthenium(II) dimer was synthesised following literature protocol.[41] ^1H NMR, $^{13}C\{^1H\}$ NMR and $^{31}P\{^1H\}$ NMR spectra were recorded on a Bruker Ultrashield 400 (^1H NMR 400.17 MHz, $^{13}C\{^1H\}$ NMR 100.62 MHz and $^{13}P\{^1H\}$ NMR 161.99 MHz) or Bruker Ultrashield 500 (^1H NMR 500.13 MHz, $^{13}C\{^1H\}$ NMR 125.75 MHz and $^{13}P\{^1H\}$ NMR 202.45 MHz) in $CDCl_3$, DMSO-d_6 and CD_2Cl_2 as appropriate at room temperature. FT-IR data was collected on PerkinElmer 83373. Elemental analyses were performed on a Thermo Scientific FLASH 2000 CHNS-O analyzer. HRMS (ESI) spectra were recorded on a Waters Synapt G2 spectrometer.

All hydrogenation reactions were performed in TAIATSU TECHNO high pressure reactor vessels with 200 °C and 10 MPa capacities fitted into a high pressure autoclave reactor (PPV-CTRO1-CE) with an in built heating, cooling and stirring systems. Conversions and hydrogenation products were determined by Bruker Ultrashield 400 (^1H NMR 400.17 MHz).

Synthesis of *N*^{1},*N*^{2}-bis(pyridin-2-ylmethylene)ethane-1,2-diamine (C1)

Compound **C1** was synthesised using a solvent-free approach. Ethylenediamine (0.025 mol; 1.68 mL) was slowly added to 2-pyridinecarboxaldehyde (0.05 mol; 4.80 mL) in a round bottom flask and the mixture was stirred at 50 °C for 1 h. After the reaction time had elapsed, the flask was allowed to cool to room temperature and the product was dried in vacuo and obtained as an orange-brown solid in excellent yield. Yield: 5.96 g (> 99%). Anal calcd. for $C_{14}H_{14}N_4$: C 70.57, H 5.92, N 23.51%; found: C 70.49, H 5.33, N 23.26%. ^1H NMR ($CDCl_3$): δ 4.04 (s, CH_2, 4H),

7.29 (dd, $^3J_{HH}$ = 1.2 Hz, $(CH)_{pyridyl}$, 2H), 7.72 (dd, $^3J_{HH}$ = 6.4 Hz, $(CH)_{pyridyl}$, 2H), 7.96 (d, $^3J_{HH}$ = 8.0 Hz, $(CH)_{pyridyl}$, 2H), 8.39 (s, CH=N, 2H), 8.60 (d, $^3J_{HH}$ = 4.8 Hz, $(CH)_{pyridyl}$, 2H).

***N*¹,*N*²-bis(pyridin-2-ylmthyl)ethane-1,2-diamine (C2)**

Compound **C2** was synthesised by adding four equivalents of $NaBH_4$ (0.1 mol; 3.78 g) to **C1** (0.025 mol; 5.96 g) dissolved in 50 mL of ethanol at room temperature. The reaction mixture was stirred at room temperature for 30 min followed by reflux at 80 °C for 2 h. After the reaction time had elapsed, aqueous solution of KOH (5.0 g in 50 mL water) was added to the crude mixture and the product extracted from the aqueous mixture using100 mL of ethyl acetate. The ethyl acetate extract was then washed with 50 mL of water. The organic phase was dried over anhydrous $MgSO_4$ and filtered through a filter paper followed by evaporation of the solvent to obtain a reddish-brown oil. Yield: 5.94 g (98%). Anal calcd. for $C_{14}H_{18}N_4$: C 69.39, H 7.49, N 23.12%; found: C 69.17, H 7.27, N 23.06%. ^{1}H NMR ($CDCl_3$): δ 1.96 (s, NH, 2H), 2.79 (s, CH_2, 4H), 3.89 (s, $(CH_2)_{pyridyl}$, 4H), 7.14 (t, $^3J_{HH}$ = 5.2 Hz, $(CH)_{pyridyl}$, 2H), 7.30 (d, $^3J_{HH}$ = 7.6 Hz, $(CH)_{pyridyl}$, 2H), 7.62 (t, $^3J_{HH}$ = 6.0 Hz, $(CH)_{pyridyl}$, 2H), 8.53 (d, $^3J_{HH}$ = 4.4 Hz, $(CH)_{pyridyl}$, 2H).

***N*¹,*N*²-bis(diphenylphosphino)-*N*¹,*N*²-bis(pyridin-2-ylmethyl)ethane-1,2-diamine (L1)**

To a diethyl ether solution (50 mL) containing **C2** (10.0 mmol; 2.5 g) and stirring at 0-5 °C under argon atmosphere, was added triethylamine (40.0 mmol; 5.63 mL). The mixture was stirred for about 10 minutes followed by addition of chlorodiphenylphosphine, (20.0 mmol; 3.85 mL) in a dropwise manner. The mixture was stirred at room temperature for 3 h and the precipitates obtained were filtered off using a filter paper and washed with 20 mL of diethyl ether. The precipitates were dissolved in 50 mL of ethyl acetate and washed successively with water (3 x 50 mL) to remove the triethylamine hydrochloride salt. The organic phase was dried over anhydrous $MgSO_4$ and filtered through a filter paper. The pure product was obtained as a pale-yellow solid upon evaporation of the solvent followed by drying *in vacuo*. Yield: 3.87 g (61%). %). Anal calcd. for $C_{38}H_{36}N_4P_2$: C 74.74, H 5.94, N 9.17%; found: C 74.63, H 6.01, N 9.20%. ^{1}H NMR (400 MHz, $CDCl_3$): δ 2.98 (d, $^3J_{HH}$ = 3.6 Hz, CH_2, 2H), 2.99 (d, $^3J_{HH}$ = 4.0 Hz, CH_2, 2H), 4.11 (s, $(CH_2)_{pyridyl}$, 2H), 4.13 (s, $(CH_2)_{pyridyl}$, 2H), 6.89 (d, $^3J_{HH}$ = 7.6 Hz, $(CH)_{pyridyl}$, 2H), 7.02 (t, $^3J_{HH}$ = 5.2, $(CH)_{pyridyl}$, 2H), 7.62 (t, $^3J_{HH}$ = 6.0 Hz, $(CH)_{pyridyl}$, 2H), 7.19-7.30 (m, $(CH)_{aromatic}$, 20H) , 7.42 (t, $^3J_{HH}$ = 1.6 Hz, $(CH)_{pyridyl}$, 2H), 8.36 (d, $^3J_{HH}$ = 0.8 Hz, $(CH)_{pyridyl}$, 2H). ^{13}C{^{1}H} NMR (100.6 MHz, $CDCl_3$): δ 50.8 (dd, $^2J_{CP}$ = 17.8 Hz, $^3J_{CP}$ = 4.8 Hz, CH_2), 57.4 (d, $^2J_{CP}$ = 21.0 Hz, $(CH_2)_{pyridyl}$), 121.5 ($(CH)_{pyridyl}$), 121.8 ($(CH)_{pyridyl}$), 128.1 (d, $^2J_{CP}$ = 5.9 Hz $(CH)_{aromatic}$), 128.4 ($(CH)_{aromatic}$), 132.0 ($(CH)_{aromatic}$), 132.2 ($(CH)_{aromatic}$), 135.9 ($(CH)_{pyridyl}$), 139.5 (d, J_{CP} = 24.3 Hz, $(C\text{-}P_{aromatic})$), 148.9 ($(CH{=}N)_{pyridyl}$), 159.8 (d, $^3J_{CP}$ = 4.8 Hz, $(C{=}N)_{pyridyl}$). ^{31}P{^{1}H} NMR (162 MHz, $CDCl_3$): δ 64.9 (2P). FT-IR (powder, cm^{-1}): $\nu(CH)_{pyridyl}$ 3073-2983; $\nu(CH)_{aromatic}$ 2900-2858; ν(C=N) 1584.

Tetraethyl ethane-1,2-diylbis((pyridin-2-ylmethyl)phosphoramidite) (L2)

Compound **L2** was synthesised in a similar manner described for **L1**. To a toluene solution (50 mL) containing **C2** (2.54 mmol; 0.62 g) and stirring at 0-5 °C under argon atmosphere, was added triethylamine (10.2 mmol; 1.4 mL). The mixture was stirred for about 10 minutes followed by addition of diethyl chlorophosphite, (5.1 mmol; 0.76 mL) in a dropwise manner. The mixture was stirred at room temperature for 12 h and the mixture was filtered off to remove the triethylamine hydrochloride salt. The filtrate was dried *in vacuo* and the product was obtained as reddish-brown oil. Yield: 1.0 g (83%). Anal calcd. for $C_{22}H_{36}N_4O_4P_2$: C 54.76, H 7.52, N 11.61%; found: C 54.81, H 7.55, N 11.53%. ^{1}H NMR (400 MHz, $CDCl_3$): δ 1.17 (t, $^3J_{HH}$ = 6.8 Hz, CH_3, 12H), 2.99 (t, $^3J_{HH}$ = 5.2 Hz, CH_2, 4H), 3.68 (m, $^3J_{HH}$ = 7.6 Hz, O-CH_2, 8H), 4.21 (s, $(CH_2)_{pyridyl}$, 2H), 4.23 (s, $(CH_2)_{pyridyl}$, 2H), 7.05 (dd, $^3J_{HH}$ = 4.8 Hz, $(CH)_{pyridyl}$, 2H), 7.28 (d, $^3J_{HH}$ = 8.0, $(CH)_{pyridyl}$, 2H), 7.56 (dd, $^3J_{HH}$ = 6.0 Hz, $(CH)_{pyridyl}$, 2H), 8.43 (d, $^3J_{HH}$ = 4.0 Hz, $(CH)_{pyridyl}$, 2H). ^{13}C{^{1}H} NMR (100.6 MHz, $CDCl_3$): δ 16.9 (d, $^3J_{CP}$ = 6.0 Hz, CH_3), 43.8 (dd, $^2J_{CP}$ = 15.2 Hz, $^3J_{CP}$ = 3.0, CH_2), 50.4 (d, $^2J_{CP}$ = 19.2 Hz, $(CH_2)_{pyridyl}$), 59.2 (d, $^2J_{CP}$ = 17.2 Hz, O-CH_2), 121.5 ($(CH)_{pyridyl}$), 121.9 ($(CH)_{pyridyl}$), 136.1 ($(CH)_{pyridyl}$), 148.9 ($(CH{=}N)_{pyridyl}$), 160.1 (d, $^3J_{CP}$ = 3.0, $(C{=}N)_{pyridyl}$). ^{31}P{^{1}H} NMR (162 MHz, $CDCl_3$): δ 145.2 (2P).

[{Ru(benzene)Cl_2}$_2$L1] (1)

A dichloromethane solution (15 mL) of $[Ru(benzene)Cl_2]_2$ (0.082 mmol; 0.041 g) was mixed with a 15 mL dichloromethane solution of ligand **L1** (0.082 mmol; 0.05 g). The mixture was stirred at room temperature for 2 h and the product precipitated with hexane after concentrating the crude. The product was dried *in vacuo* to obtain reddish-brown solids. Yield: 81.0 mg (89%). M.p: decomposes without melting (onset at 189 °C). Anal calcd. for $C_{50.5}H_{49}Cl_5N_4P_2Ru_2$ (**1**·0.5CH_2Cl_2): C 52.59, H 4.28, N 4.86%;

found: C 52.12, H 4.21, N 5.01%. ^{1}H NMR (400 MHz, $CDCl_3$): δ 2.41 (m, *J* = 9.2, CH_2, 4H), 5.13 (s, $(CH)_{benzene}$, 12H), 6.95 (d, $^3J_{HH}$ = 7.6 Hz, $(CH)_{pyridyl}$, 2H), 7.20 (t, $^3J_{HH}$ = 6.8 Hz, $(CH)_{pyridyl}$, 2H), 7.22 (m, $(CH)_{aromatic}$, 12H), 7.59 (t, $^3J_{HH}$ = 7.6 Hz, $(CH)_{pyridyl}$, 2H), 7.70 (m, $(CH)_{aromatic}$, 8H), 8.62 (d, $^3J_{HH}$ = 3.6 Hz, $(CH)_{pyridyl}$, 2H). $^{13}C\{^1H\}$ NMR (100.6 MHz, CD_2Cl_2): δ 47.1 (CH_2), 55.4 ($(CH_2)_{pyridyl}$), 89.8 (d, $^3J_{CP}$ = 10.0 Hz, benzene-CH), 122.8 ($(CH)_{pyridyl}$), 122.9 ($(CH)_{aromatic}$), 127.9($(CH)_{pyridyl}$), 130.4 ($(CH)_{aromatic}$), 133.1 ($(CH)_{aromatic}$), 136.9 ($(CH)_{pyridyl}$), 150.0 ($(CH=N)_{pyridyl}$), 159.9 $(C=N)_{pyridyl}$). $^{31}P\{^1H\}$ NMR (162 MHz, $CDCl_3$): δ 75.9 (N-P-Ru, 2P). FT-IR (powder, cm^{-1}): *ν*$(CH)_{pyridyl}$ 3058; *ν*$(CH)_{aromatic}$ 2954-2856; *ν*(C=N) 1588. HRMS (ESI^+): m/z: 521.0454 [**1**-2Cl]$^{2+}$.

[{Ru(*p*-cymene)Cl$_2$}$_2$L1] (2)

Complex **2** was synthesised in a similar manner described for **1** using **L1** (0.082 mmol; 0.05 g) and [Ru(*p*-cymene)Cl_2]$_2$ (0.082 mmol, 0.05 g). The mixture was stirred in 30 mL of dichloromethane at room temperature for 2 h. The product was precipitated with hexane after concentrating the crude and dried under vacuum to obtain the pure product as a reddish-brown solid. Yield: 0.085 g (85%). M.p: decomposes without melting (onset at 190 °C). Anal calcd. for $C_{58.5}H_{65}Cl_5N_4P_2Ru_2$ (**2**·0.5CH_2Cl_2): C 55.52, H 5.18, N 4.43%; found: C 55.20, H 5.22, N 4.38%. ^{1}H NMR (400 MHz, CD_2Cl_2): δ 0.88 (d, *J* = 6.8, *p*-cym-C-$(CH_3)_2$, 12H), 1.23 (s, *p*-cym-CH_3, 6H), 2.03 (m, $^3J_{HH}$ = 6.8 Hz, *p*-cym-$CH(CH_3)_2$), 2H), 2.20 (s, CH_2, 4H), 4.38 (s, $(CH_2)_{pyridyl}$, 4H), 5.09 (d, $^3J_{HH}$ = 5.2 Hz, *p*-cym-CH, 4H), 5.19 (d, $^3J_{HH}$ = 5.2 Hz, *p*-cym-CH, 4H), 6.98 (d, $^3J_{HH}$ = 7.6 Hz, $(CH)_{pyridyl}$, 2H), 7.23 (m, $(CH)_{aromatic}$, 12H), 7.59 (t, $^3J_{HH}$ = 7.6, $(CH)_{pyridyl}$, 2H), 7.70 (m, $(CH)_{aromatic}$, 8H), 8.64 (d, $^3J_{HH}$ = 2.4 Hz, $(CH)_{pyridyl}$, 2H). $^{13}C\{^1H\}$ NMR (100.6 MHz, CD_2Cl_2): δ 16.5 (*p*-cym-CH_3,), 22.2 (*p*-cym-CH($\underline{C}H_3$)$_2$), 30.2 (*p*-cym-$\underline{C}H(CH_3)_2$), 46.9 (CH_2), 54.3 ($(CH_2)_{pyridyl}$), 86.0 (*p*-cym-CH), 91.1 (*p*-cym-CH), 96.3 (*p*-cym-C_q), 109.4 (*p*-cym-Cq), 122.6 ($(CH)_{aromatic}$), 122.9 ($(CH)_{pyridyl}$), 127.8 ($(CH)_{aromatic}$), 130.1($(CH)_{pyridyl}$), 133.2 ($(CH)_{aromatic}$), 136.8 ($(CH)_{pyridyl}$), 149.9 ($(CH=N)_{pyridyl}$), 160.0 $(C=N)_{pyridyl}$). $^{31}P\{^1H\}$ NMR (162 MHz, CD_2Cl_2): δ 73.4 (N-P-Ru, 2P). FT-IR (powder, cm^{-1}): *ν*$(CH_{pyridyl})$ 3046-2962; *ν*$(CH)_{aromatic}$ 2924-2866; *ν*(C=N) 1587. HRMS (ESI^+): m/z: 576.1054 [**2**-2Cl]$^{2+}$; 1189.1929 [**2**-Cl]$^+$.

[{Ru(benzene)Cl$_2$}$_2$L2] (3)

Complex **3** was synthesised in a similar manner described for **1** using **L2** (0.37 mmol; 0.18 g) and [Ru(benzene)Cl_2]$_2$ (0.37 mmol; 0.19 g). The mixture was stirred in 40 mL of dichloromethane at room temperature for 2 h and the product precipitated with hexane after concentrating the crude. The product was dried *in vacuo* to obtain a reddish-brown solid. Yield: 0.35 g (97%). M.p: decomposes without melting (onset at 175 °C). Anal calcd. for $C_{34}H_{48}Cl_4N_4O_4P_2Ru_2$ (**3**): C 41.56, H 4.92, N 5.70%; found: C 41.83, H 4.90, N 5.74%. ^{1}H NMR (400 MHz, $CDCl_3$): δ 1.12 (t, $^3J_{HH}$ = 7.2 Hz, CH_3, 12H), 3.35 (t, $^3J_{HH}$ = 4.4 Hz, CH_2, 4H), 3.88 (m, $^3J_{HH}$ = 3.2 Hz, O-CH_2, 4H), 4.03 (m, $^3J_{HH}$ = 3.2 Hz, O-CH_2, 4H), 4.51 (s, $(CH_2)_{pyridyl}$, 2H), 4.54 (s, $(CH_2)_{pyridyl}$, 2H), 5.70 (s, $(CH)_{benzene}$), 7.14 (dd, $^3J_{HH}$ = 5.2 Hz, $(CH)_{pyridyl}$, 2H), 7.39 (d, $^3J_{HH}$ = 7.6, $(CH)_{pyridyl}$, 2H), 7.63 (dd, $^3J_{HH}$ = 6.8 Hz, $(CH)_{pyridyl}$, 2H), 8.51 (d, $^3J_{HH}$ = 4.0 Hz, $(CH)_{pyridyl}$, 2H). $^{13}C\{^1H\}$ NMR (100.6 MHz, $CDCl_3$): δ 16.0 (CH_3), 45.0 (CH_2), 49.0 ($(CH_2)_{pyridyl}$), 62.7 (O-CH_2), 90.2 (q, $^2J_{CP}$ = 6.1 Hz, $(CH)_{benzene}$), 122.1 ($(CH)_{pyridyl}$), 122.7 ($(CH)_{pyridyl}$), 136.5 ($(CH)_{pyridyl}$), 149.1 ($(CH=N)_{pyridyl}$), 161.2 (d, $^3J_{CP}$ = 3.0, $(C=N)_{pyridyl}$). $^{31}P\{^1H\}$ NMR (162 MHz, $CDCl_3$): δ 120.5 (N-P-Ru, 2P). FT-IR (powder, cm^{-1}): *ν*$(CH)_{pyridyl}$ 3069-2977; *ν*$(CH)_{aromatic}$ 2931; *ν*(C=N) 1590. HRMS (ESI^+): m/z: 456.0316 [**3**-2Cl]$^{2+}$.

[{Ru(*p*-cymene)Cl$_2$}$_2$L2] (4)

Complex **4** was synthesised in a similar manner described for **1** using **L2** (0.68 mmol; 0.33 g) and [Ru(*p*-cymene)Cl_2]$_2$ (0.68 mmol; 0.43 g). The mixture was stirred in 40 mL of dichloromethane at room temperature for 2 h and the product precipitated with hexane after concentrating the crude. The product was dried *in vacuo* to obtain a reddish-brown solid. Yield: 0.71 g (95%). M.p: decomposes without melting (onset at 180 °C). Anal calcd. for $C_{42.5}H_{65}Cl_5N_4O_4P_2Ru_2$ (**4**·0.5CH_2Cl_2): C 44.88, H 5.76, N 4.93%; found: C 45.13, H 5.72, N 5.01%. ^{1}H NMR (400 MHz, $CDCl_3$): δ 1.08 (t, $^3J_{HH}$ = 7.2 Hz, CH_3, 12H), 1.18 (d, $^3J_{HH}$ = 6.8, *p*-cym-C-$(CH_3)_2$, 6H), 1.22 (d, $^3J_{HH}$ = 6.8 Hz, *p*-cym-$CH(CH_3)_2$, 6H), 2.08 (s, *p*-cym-CH_3, 6H), 2.92 (m, $^3J_{HH}$ = 6.8 Hz, *p*-cym-$CH(CH_3)_2$), 2H), 3.31 (d, $^3J_{HH}$ = 2.8 Hz, CH_2, 4H), 3.99 (m, $^3J_{HH}$ = 6.4 Hz, O-CH_2, 8H), 4.46 (d, $^2J_{HH}$ = 10.4 Hz, $(CH_2)_{pyridyl}$, 4H), 5.44 (d, $^3J_{HH}$ = 6.0 Hz, *p*-cym-CH, 4H), 5.53 (d, $^3J_{HH}$ = 6.0 Hz, *p*-cym-CH, 4H), 7.10 (dd, $^3J_{HH}$ = 5.6 Hz, $(CH)_{pyridyl}$, 2H), 7.50 (d, $^3J_{HH}$ = 7.6, $(CH)_{pyridyl}$, 2H), 7.61 (dd, $^3J_{HH}$ = 6.8, $(CH)_{pyridyl}$, 2H), 8.48 (d, $^3J_{HH}$ = 4.4 Hz, $(CH)_{pyridyl}$, 2H). $^{13}C\{^1H\}$ NMR (100.6 MHz, $CDCl_3$): δ 15.6 (CH_3), 15.8 (CH_3), 17.4 (*p*-cym-CH_3,), 21.4 (*p*-cym-CH($\underline{C}H_3$)$_2$), 21.9 (*p*-cym-CH($\underline{C}H_3$)$_2$), 30.4 (*p*-cym-$\underline{C}H(CH_3)_2$), 45.8 (CH_2), 46.2 (CH_2), 52.3 ($(CH_2)_{pyridyl}$), 52.7 ($(CH_2)_{pyridyl}$), 61.4 (d, $^2J_{CP}$ = 12.1 Hz, O-CH_2), 62.4 (O-CH_2), 89.9 (*p*-cym-CH), 90.9 (*p*-cym-CH), 91.2 (*p*-cym-CH), 93.3 (*p*-cym-CH), 102.8 (d, $^3J_{CP}$ = 9.1 Hz, *p*-cym-Cq), 111.76 (*p*-cym-Cq), 124.4 ($(CH)_{pyridyl}$), 126.0 ($(CH)_{pyridyl}$), 139.4 ($(CH)_{pyridyl}$),

158.0 ($(CH=N)_{pyridyl}$), 158.4 ($(CH=N)_{pyridyl}$), 160.4 ($(C=N)_{pyridyl}$). $^{31}P\{^1H\}$ NMR (162 MHz, $CDCl_3$): δ 122.5 (N-P-Ru, 2P). FT-IR (powder, cm^{-1}): *ν*$(CH)_{pyridyl}$ 3063-2972; *ν*$(CH)_{aromatic}$ 2926-2875; *ν*(C=N) 1586. HRMS (ESI^+): m/z: 513.0943 [**4**-2Cl]$^{2+}$;1057.1572 [**4**-Cl]$^+$.

[{Ru(benzene)Cl}$_2$L1]2BPh$_4$ (5a and 5b)

A dichloromethane solution (15 mL) of $[Ru(benzene)Cl_2]_2$ (0.164 mmol; 0.082 g) was mixed with a 15 mL dichloromethane solution of ligand **L1** (0.164 mmol; 0.10 g). The mixture was stirred at room temperature for 2 h after which $NaBPh_4$ (0.33 mmol; 0.112 g) in 4 mL of methanol was added and stirred for 16 h. The crude was washed with 20 mL portions of water three times and dried over anhydrous $MgSO_4$. The product in the dichloromethane solution was then precipitated with diethyl ether as an orange-yellow solid and dried under vacuum, resulting in a total yield of 0.26 g (95%). Compound **5b** was extracted into acetone by washing the mixture with about 15 x 3 mL portions of acetone, leaving **5a** behind. (**5a**): Yield 0.11 g (40%); M.p: decomposes without melting (onset at 205 °C). Anal calcd. for $C_{98}H_{88}Cl_2N_4P_2B_2Ru_2$ (**5a**): C 70.23, H 5.28, N 3.34%; found: C 69.83, H 5.44, N 3.45%. ^1H NMR (400 MHz, Acetonitrile-d_3): δ 2.47 (t, $^2J_{HH}$ = 5.2 Hz CH_2, 2H), 2.99-3.11 (q, $^2J_{HH}$ = 16.0 Hz, $(CH_2)_{pyridyl}$, 2H), 3.937-3.991 (dd, $^2J_{HH}$ = 10.4 Hz; $^2J_{HH}$ = 5.2 Hz, $(CH_2)_{pyridinyl}$, 2H), 5.41 (s, $(CH)_{benzene}$, 12H), 6.63 (t, $^3J_{HH}$ = 8.0 Hz, $(CH)_{aromatic}$, 4H), 6.84 (t, $^3J_{HH}$ = 6.8 Hz, $(CH)_{aromatic}$, 8H), 6.959-6.99 (m, $(CH)_{BPh4}$, 16H), 7.24-7.26 (bm, $(CH)_{BPh4}$, 18H), 7.38 (t, $^3J_{HH}$ = 8.8 Hz, $(CH)_{pyridyl}$, 2H), 7.51 (d, $^3J_{HH}$ = 4.8 Hz, $(CH)_{pyridyl}$, 1H), 7.69-7.71 (m, $(CH)_{aromatic}$, 6H), 7.85 (t, $^3J_{H-H}$ = 7.6 Hz, $(CH)_{pyridyl}$, 2H), 9.41 (d, $^3J_{HH}$ = 5.6 Hz, $(CH)_{pyridyl}$, 2H). $^{13}C\{^1H\}$ NMR (100.6 MHz, DMSO-d_6): δ 48.9 (CH_2), 49.9 (CH_2), 57.6 ($(CH_2)_{pyridyl}$), 57.8 ($(CH_2)_{pyridyl}$), 92.4 (q, $^3J_{C-P}$ = 6.5 Hz, benzene-CH), 121.5 ($(CH)_{aromatic}$), 121.5 ($(CH)_{BPh4}$), 124.6 ($(CH)_{aromatic}$), 124.8 ($(CH)_{pyridyl}$), 125.2-125.3 ($(CH)_{BPh4}$), 127.9 ($(CH)_{BPh4}$,) 127.2 ($(CH)_{aromatic}$), 127.4 ($(CH)_{pyridyl}$), 128.3 ($(CH)_{aromatic}$), 129.9 ($(Cq)_{BPh4}$,) 130.3 ($(CH)_{pyridyl}$), 130.7 ($(CH)_{aromatic}$), 131.2 ($(CH)_{aromatic}$), 132.5 ($(Cq)_{aromatic}$), 133.4 ($(Cq)_{BPh4}$,), 135.5 ($(CH)_{BPh4}$), 140.0 ($(CH)_{pyridyl}$), 158.4 ($(CH)_{aromatic}$), 161.4 ($(CH=N)_{pyridyl}$), 161.5 ($C=N)_{pyridyl}$), 162.8 (q, J_{CB} = 49.5 Hz, $(C-B)_{BPh4}$). $^{31}P\{^1H\}$ NMR (162 MHz, acetonitrile-d_3): δ 85.8 (N-P-Ru, 1P). FT-IR (powder, cm^{-1}): *ν*$(CH)_{pyridyl}$ 3054-2987; *ν*(C=N) 1603. HRMS (ESI^+): m/z: 521.0374 $[C_{50}H_{48}Cl_2N_4P_2Ru_2]^{2+}$; HRMS ($ESI^-$): *m/z* 319.1749 BPh_4^-.

(**5b**): Yield: 0.094 g (34%); M.p: decomposes without melting (onset at 202 °C); Anal calcd. for $C_{98}H_{88}Cl_2N_4P_2B_2Ru_2$ (**5b**): C 70.23, H 5.28, N 3.34%; found: C 70.11, H 5.39, N 3.28%. ^1H NMR (400 MHz, Acetonitrile-d_3): δ 2.65 (t, $^2J_{HH}$ = 8.8 Hz CH_2, 2H), 3.67-3.73 (q, $^2J_{HH}$ = 16.0 Hz, $(CH_2)_{pyridyl}$, 2H), 4.08-4.13 (dd, $^2J_{HH}$ = 12.4 Hz; $^2J_{HH}$ = 3.6 Hz, $(CH_2)_{pyridinyl}$, 2H), 5.40 (s, $(CH)_{benzene}$, 12H), 6.24 (t, $^3J_{HH}$ = 10.4 Hz, $(CH)_{aromatic}$, 4H), 6.82 (t, $^3J_{HH}$ = 7.2 Hz, $(CH)_{aromatic}$, 8H), 6.95-6.99 (m, $(CH)_{BPh4}$, 16H), 7.25-7.26 (bm, $(CH)_{BPh4}$, 18H), 7.38 (t, $^3J_{HH}$ = 8.8 Hz, $(CH)_{pyridyl}$, 2H), 7.45 (d, $^3J_{HH}$ = 7.2 Hz, $(CH)_{pyridyl}$, 2H), 7.71-7.84 (m, $(CH)_{aromatic}$, 6H), 7.89 (t, $^3J_{H-H}$ = 7.6 Hz, $(CH)_{pyridyl}$, 2H), 9.34 (d, $^3J_{HH}$ = 5.2 Hz, $(CH)_{pyridyl}$, 2H). $^{13}C\{^1H\}$ NMR (100.6 MHz, DMSO-d_6): δ 48.9 (CH_2), 49.9 (CH_2), 57.6 ($(CH_2)_{pyridyl}$), 57.8 ($(CH_2)_{pyridyl}$), 92.4 (q, $^3J_{C-P}$ = 6.5 Hz, benzene-CH), 121.5 ($(CH)_{aromatic}$), 121.5 ($(CH)_{BPh4}$), 124.6 ($(CH)_{aromatic}$), 124.8 ($(CH)_{pyridyl}$), 125.2-125.3 ($(CH)_{BPh4}$), 127.9 ($(CH)_{BPh4}$,) 127.2 ($(CH)_{aromatic}$), 127.4 ($(CH)_{pyridyl}$), 128.3 ($(CH)_{aromatic}$), 129.9 ($(Cq)_{BPh4}$,) 130.3 ($(CH)_{pyridyl}$), 130.7 ($(CH)_{aromatic}$), 131.2 ($(CH)_{aromatic}$), 132.5 ($(Cq)_{aromatic}$), 133.4 ($(Cq)_{BPh4}$,), 135.5 ($(CH)_{BPh4}$), 140.0 ($(CH)_{pyridyl}$), 158.4 ($(CH)_{aromatic}$), 161.4 ($(CH=N)_{pyridyl}$), 161.5 ($C=N)_{pyridyl}$), 162.8 (q, J_{CB} = 49.5 Hz, $(C-B)_{BPh4}$). $^{31}P\{^1H\}$ NMR (162 MHz, acetonitrile-d_3): δ 85.8 (N-P-Ru, 1P). FT-IR (powder, cm^{-1}): *ν*$(CH)_{pyridyl}$ 3054-2987; *ν*(C=N) 1603. HRMS (ESI^+): m/z: 521.0374 $[C_{50}H_{48}Cl_2N_4P_2Ru_2]^{2+}$; HRMS ($ESI^-$): *m/z* 319.1749 BPh_4^-

[{Ru(*p*-cymene)Cl}$_2$L1]2BPh$_4$ (6a and 6b)

Complexes **6a** and **6b** were synthesised in a similar manner described for **5a** and **5b** using **L1** (0.33 mmol, 0.20 g), $[Ru(p\text{-cymene})Cl_2]_2$ (0.33 mmol, 0.20 g) and $NaBPh_4$ (0.65 mmol, 0.224 g). The mixture of the isomers was obtained as an orange-yellow solid after precipitation with diethyl ether with total yield of 0.51 g (87%). Washing of the mixture with 30 mL of dichloromethane in 3 mL portions resulted in the separation of **6b** from **6a**. (**6a**): Yield: 0.23 g (39%) M.p: decomposes without melting (onset at 226 °C). Anal calcd. for $C_{106.5}H_{105}Cl_3N_4P_2B_2Ru_2$ (**6a**·0.5CH_2Cl_2): C 69.78, H 5.77, N 3.06%; found: C 69.53, H 5.74, N 2.88%. ^1H NMR (400 MHz, Acetone-d6): δ 0.96 (d, $^3J_{HH}$ = 6.8 Hz, *p*-cym-C-$(CH_3)_2$, 6H), 1.19 (d, $^3J_{HH}$ = 6.8 Hz, *p*-cym-C-$(CH_3)_2$, 6H), 1.67 (s, *p*-cym-CH_3, 6H), 2.28 (bd, $^3J_{HH}$ = 7.0 Hz, (CH_2), 2H), 2.63 (m, $^3J_{HH}$ = 6.8 Hz, *p*-cym-$CH(CH_3)_2$), 2H), 2.72 (bd, $^3J_{HH}$ = 8.0 Hz, (CH_2), 2H), 3.551-3.664 (q, $^2J_{HH}$ = 15.6 Hz, $(CH_2)_{pyridyl}$, 2H), 4.24-4.29 (dd, $^2J_{HH}$ = 10.0 Hz; 5.6 Hz, $(CH_2)_{pyridyl}$, 2H), 5.04 (d, $^3J_{HH}$ = 6.4 Hz, *p*-cym-CH, 2H), 5.09 (d, $^3J_{HH}$ = 6.4 Hz, *p*-cym-CH, 2H), 5.42 (d, $^3J_{HH}$ = 6.0 Hz, *p*-cym-CH, 2H), 5.94 (d, $^3J_{HH}$ = 6.0 Hz, *p*-cym-CH, 2H), 6.72-6.78 (m, $(CH)_{aromatic}$, 12H), 6.92 (t, $^3J_{HH}$ = 7.6 Hz, $(CH)_{BPh4}$, 16H), 7.21-7.24 (m, $(CH)_{aromatic}$, 4H), 7.26 (t, $^3J_{HH}$ = 2.4 Hz, $(CH)_{pyridyl}$, 2H),

7.30-7.34 (bm, $(CH)_{BPh4}$, 20H), 7.60 (t, $^3J_{HH}$ = 8.4, $(CH)_{pyridyl}$, 2H), 7.60-7.66 (m, $(CH)_{aromatic}$, 4H), 7.75-7.76 (m, $(CH)_{aromatic}$, 6H), 7.95 (t, $^3J_{HH}$ = 6.0 Hz, $(CH)_{pyridyl}$, 2H), 9.44 (d, $^3J_{HH}$ = 5.2 Hz, $(CH)_{pyridyl}$, 2H). $^{13}C\{^1H\}$ NMR (100.6 MHz, DMSO-d_6): δ 16.9 (*p*-cym-CH_3,), 21.0 (*p*-cym-CH($\underline{C}H_3$)$_2$), 21.1 (*p*-cym-CH($\underline{C}H_3$)$_2$), 30.2 (*p*-cym-$\underline{C}H(CH_3)_2$), 54.9 (CH_2), 55.9 ($(CH_2)_{pyridyl}$), 88.3 (*p*-cym-CH), 91.7 (*p*-cym-CH), 92.4 (*p*-cym-CH), 93.9 (d, $^3J_{C\text{-}P}$ = 6.1 Hz, *p*-cym-CH), 100.0 (*p*-cym-C_q), 113.0 (*p*-cym-Cq), 121.5 ($(CH)_{aromatic}$), 124.7 ($(CH)_{pyridyl}$), 125.2-125.3 ($(CH)_{BPh4}$), 127.3 ($(CH)_{BPh4}$), 127.9 ($(Cq)_{BPh4}$,) 129.1 ($(CH)_{aromatic}$), 130.4($(CH)_{pyridyl}$), 130.6 ($(CH)_{pyridyl}$), 131.3 ($(CH)_{aromatic}$), 132.3 ($(CH)_{aromatic}$), 133.0 ($(Cq)_{aromatic}$), 135.5 ($(Cq)_{BPh4}$,), 140.1 ($(CH)_{pyridyl}$), 158.6 ($(CH)_{aromatic}$), 161.4 ($(CH{=}N)_{pyridyl}$), 161.5 ($C{=}N)_{pyridyl}$), 164.1 (q, J_{CB} = 49.5 Hz, (C-B)$_{BPh4}$). $^{31}P\{^1H\}$ NMR (162 MHz, acetone-d6): δ 87.6 (N-P-Ru, 2P). FT-IR (powder, cm^{-1}): $\nu(CH)_{pyridyl}$ 3055-2984; $\nu(CH)_{aromatic}$ 2900-2858; ν(C=N) 1605. HRMS (ESI^+): m/z: 576.1044 $[C_{58}H_{64}Cl_2N_4P_2Ru_2]^{2+}$; HRMS ($ESI^-$): *m/z* 319.1746 BPh_4^-.

(**6b**): Yield: 0.21 g (35%) M.p: decomposes without melting (onset at 225 °C); Anal calcd. for $C_{106.5}H_{105}Cl_3N_4P_2B_2Ru_2$ (**6b**·0.5CH_2Cl_2): C 69.78, H 5.77, N 3.06%; found: C 69.53, H 5.74, N 2.88%. ^1H NMR (400 MHz, Acetone-d6): δ 0.96 (d, $^3J_{HH}$ = 7.2 Hz, *p*-cym-C-$(CH_3)_2$, 6H), 1.18 (d, $^3J_{HH}$ = 6.8 Hz, *p*-cym-C-$(CH_3)_2$, 6H), 1.71 (s, *p*-cym-CH_3, 6H), 2.27 (m, $^3J_{HH}$ = 7.6 Hz, (CH_2), 2H), 2.60 (m, $^3J_{HH}$ = 6.8 Hz, *p*-cym-CH$(CH_3)_2$), 2H), 2.91 (dd, $^3J_{HH}$ = 8.8 Hz, (CH_2), 2H), 3.91-4.02 (q, $^2J_{HH}$ = 15.6 Hz, $(CH_2)_{pyridyl}$, 2H), 4.30-4.35 (dd, $^2J_{HH}$ = 11.6 Hz; 4.4 Hz, $(CH_2)_{pyridyl}$, 2H), 4.98 (d, $^3J_{HH}$ = 6.0 Hz, *p*-cym-CH, 2H), 5.06 (d, $^3J_{HH}$ = 6.4 Hz, *p*-cym-CH, 2H), 5.27 (d, $^3J_{HH}$ = 6.4 Hz, *p*-cym-CH, 2H), 5.88 (d, $^3J_{HH}$ = 5.6 Hz, *p*-cym-CH, 2H), 6.39 (q, $^3J_{HH}$ = 8.4 Hz, $(CH)_{aromatic}$, 4H), 6.78 (t, $^3J_{HH}$ = 7.2 Hz, $(CH)_{aromatic}$, 12H), 6.92 (t, $^3J_{HH}$ = 7.6 Hz, $(CH)_{BPh4}$, 16H), 7.06-7.10 (m, $(CH)_{aromatic}$, 4H), 7.26 (t, $^3J_{HH}$ = 7.6 Hz, $(CH)_{pyridyl}$, 2H), 7.32-7.33 (bm, $(CH)_{BPh4}$, 20H), 7.52 (t, $^3J_{HH}$ = 6.4, $(CH)_{pyridyl}$, 2H), 7.81-7.87 (m, $(CH)_{aromatic}$, 10H), 7.96 (t, $^3J_{HH}$ = 6.4 Hz, $(CH)_{pyridyl}$, 2H), 9.36 (d, $^3J_{HH}$ = 5.6 Hz, $(CH)_{pyridyl}$, 2H). $^{13}C\{^1H\}$ NMR (100.6 MHz, Acetone-d6): δ 17.6 (*p*-cym-CH_3,), 21.8 (*p*-cym-CH($\underline{C}H_3$)$_2$), 22.0 (*p*-cym-CH($\underline{C}H_3$)$_2$), 31.5 (*p*-cym-$\underline{C}H(CH_3)_2$), 51.0 (CH_2), 58.6 (dd, $^3J_{C\text{-}P}$ = 4.0 Hz, $(CH_2)_{pyridyl}$), 88.5 (*p*-cym-CH), 92.8 (*p*-cym-CH), 93.9 (*p*-cym-CH), 94.6 (d, $^3J_{C\text{-}P}$ = 7.0 Hz, *p*-cym-CH), 100.8 (*p*-cym-C_q), 116.5 (*p*-cym-Cq), 122.1 ($(CH)_{aromatic}$), 125.8-125.9 ($(CH)_{BPh4}$), 126.1 ($(CH)_{pyridyl}$), 128.4 ($(CH)_{aromatic}$), 130.1($(CH)_{pyridyl}$), 131.7 ($(CH)_{pyridyl}$), 134.1 ($(CH)_{aromatic}$), 134.7 ($(CH)_{aromatic}$), 136.9 ($(Cq)_{aromatic}$), 136.9 ($(Cq)_{BPh4}$,), 140.9 ($(CH)_{pyridyl}$), 159.7 ($(CH)_{aromatic}$), 161.6 ($(CH{=}N)_{pyridyl}$), 161.7 ($C{=}N)_{pyridyl}$), 165.5 (q, J_{CB} = 49.3 Hz, (C-B)$_{BPh4}$). $^{31}P\{^1H\}$ NMR (162 MHz, acetone-d6): δ 87.3 (N-P-Ru, 2P). FT-IR (powder, cm^{-1}): $\nu(CH)_{pyridyl}$ 3055-2984; $\nu(CH)_{aromatic}$ 2900-2858; ν(C=N) 1605. HRMS (ESI^+): m/z: 576.1051 $[C_{58}H_{64}Cl_2N_4P_2Ru_2]^{2+}$; HRMS ($ESI^-$): *m/z* 319.1746 BPh_4^-.

[{Ru(*p*-benzene)Cl}$_2$L2]2BPh$_4$ (7a and 7b)

Complexes **7a** and **7b** were synthesised in a similar manner described for **5a** and **5b** using **L2** (0.46 mmol; 0.22 g), $[Ru(benzene)Cl_2]_2$ (0.46 mmol; 0.23 g) and $NaBPh_4$ (0.92 mmol; 0.31 g). The pure product was obtained as an orange-yellow solid in good yield. Yield: 0.62 g (87%); Anal calcd. for $C_{82.5}H_{89}Cl_3N_4O_4P_2B_2Ru_2$ (**7**·0.5CH_2Cl_2): C 62.21, H 5.63, N 3.52%; found: C 62.15, H 5.68, N 3.51%; M.p: (152.4-153.1 °C). ^1H NMR (400 MHz, DMSO-d6): δ 1.35 (t, $^3J_{HH}$ = 4.4 Hz, CH_3, 6H), 1.44 (t, $^3J_{HH}$ = 7.2 Hz, CH_3, 6H), 2.49 (d, CH_2, 2H), 2.80 (d, CH_2, 2H), 3.88 (dd, $^3J_{HH}$ = 5.6 Hz, $(CH_2)_{pyridyl}$, 2H), 3.96-4.17 (m, $^3J_{HH}$ = 5.2 Hz, O-CH_2, 8H), 4.31 (dd, $^3J_{HH}$ = 14.0 Hz, $(CH_2)_{pyridyl}$, 2H), 5.95 (s, $(CH)_{benzene}$), 6.80 (d, $^3J_{HH}$ = 5.2 Hz, $(CH)_{BPh4}$, 8H), 6.93 (t, $^3J_{HH}$ = 4.8 Hz, $(CH)_{BPh4}$, 16H), 7.18 (bs, $(CH)_{BPh4}$, 16H), 7.39 (dd, $^3J_{HH}$ = 10.0 Hz, $(CH)_{pyridyl}$, 2H), 7.72 (d, $^3J_{HH}$ = 5.6, $(CH)_{pyridyl}$, 2H), 8.02 (dd, $^3J_{HH}$ = 5.6 Hz, $(CH)_{pyridyl}$, 2H), 9.29 (d, $^3J_{HH}$ = 11.6 Hz, $(CH)_{pyridyl}$, 2H). $^{13}C\{^1H\}$ NMR (100.6 MHz, DMSO-d_6): δ 15.6 (CH_3), 15.9 (CH_3), 45.6 (CH_2), 52.3 ($(CH_2)_{pyridyl}$), 61.3 (d, $^2J_{CP}$ = 11.1 Hz, O-CH_2), 62.6 (O-CH_2), 92.4 (d, $^2J_{CP}$ = 3.0 Hz, $(CH)_{benzene}$), 121.5 ($(CH)_{BPh4}$), 124.1 ($(CH)_{pyridyl}$), 125.3 ($(CH)_{BPh4}$), 128.3 ($(CH)_{pyridyl}$), 135.5 ($(CH)_{BPh4}$), 139.3 ($(CH)_{pyridyl}$), 158.7 ($(CH{=}N)_{pyridyl}$), 160.3 ($(C{=}N)_{pyridyl}$), 164.1 (q, J_{CB} = 49.5 Hz, (C-B)$_{BPh4}$). $^{31}P\{^1H\}$ NMR (162 MHz, DMSO-d_6): δ 129.3 (N-P-Ru, 1P), 129.9 (N-P-Ru, 1P). FT-IR (powder, cm^{-1}): $\nu(CH)_{pyridyl}$ 3055-2983; $\nu(CH)_{aromatic}$ 2900; ν(C=N) 1606. HRMS (ESI^+): m/z: 456.0303 $[C_{36}H_{56}Cl_2N_4O_4P_2Ru_2]^{2+}$; HRMS ($ESI^-$): *m/z* 319.1671 BPh_4^-.

[{Ru(*p*-cymene)Cl}$_2$L2]2BPh$_4$ (8a and 8b)

Complexes **8a** and **8b** were synthesised in a similar manner described for **7a** and **7b** using **L2** (0.64 mmol; 0.31 g), $[Ru(p\text{-cymene})Cl_2]_2$ (0.64 mmol; 0.39 g) and $NaBPh_4$ (1.28 mmol; 0.44 g). The pure product was obtained as a dark-brown solid after precipitation with diethyl ether. Yield: 0.87 g (82%); M.p: (129.6-130.8 °C); Anal calcd. for $C_{90.5}H_{105}Cl_3N_4O_4P_2B_2Ru_2$ (**8**·0.5CH_2Cl_2): C 63.76, H 6.21, N 3.29%; found: C 63.90, H 5.85, N 3.20%. ^1H NMR (400 MHz, DMSO-d_6): δ 0.96 (d, $^3J_{HH}$ = 6.8, *p*-cym-C-$(CH_3)_2$, 6H), 1.13 (d, $^3J_{HH}$ = 6.8 Hz, *p*-cym-C-$(CH_3)_2$, 6H), 1.24 (t, $^3J_{HH}$ = 8.0 Hz, CH_3, 6H), 1.35 (t, $^3J_{HH}$ = 4.8 Hz, CH_3, 6H), 1.80 (s, *p*-cym-CH_3, 3H), 1.82 (s, *p*-cym-CH_3, 3H), 2.27 (t, $^3J_{HH}$ = 7.6 Hz, CH_2,

2H), 2.65 (t, $^3J_{HH}$ = 8.4 Hz, *p*-cym-CH(CH_3)$_2$), 2H), 2.78 (t, CH_2, 2H), 3.81-3.98 (m, $(CH_2)_{pyridyl}$, 4H), 4.00-4.281 (m, $^3J_{H-H}$ = 5.2 Hz, O-CH_2, 8H), 5.90 (d, $^3J_{HH}$ = 6.4 Hz, *p*-cym-CH, 2H), 5.97 (d, $^3J_{HH}$ = 6.8 Hz, *p*-cym-CH, 4H), 6.07 (d, $^3J_{HH}$ = 5.2 Hz, *p*-cym-CH, 2H), 6.80 (t, $^3J_{HH}$ = 7.2 Hz, $(CH)_{BPh4}$, 8H), 6.94 (t, $^3J_{H-H}$ = 7.2 Hz, $(CH)_{BPh4}$, 16H), 7.18 (bs, $(CH)_{BPh4}$, 16H), 7.43 (dd, $^3J_{HH}$ = 7.2 Hz, $(CH)_{pyridyl}$, 2H), 7.55 (d, $^3J_{HH}$ = 7.6, $(CH)_{pyridyl}$, 1H), 7.70 (d, $^3J_{HH}$ = 7.2, $(CH)_{pyridyl}$, 1H), 7.97 (dd, $^3J_{HH}$ = 7.2 Hz, $(CH)_{pyridyl}$, 1H), 8.03 (dd, $^3J_{HH}$ = 8.0 Hz, $(CH)_{pyridyl}$, 1H), 9.20 (d, $^3J_{HH}$ = 6.0 Hz, $(CH)_{pyridyl}$, 1H), 9.21 (d, $^3J_{HH}$ = 6.4 Hz, $(CH)_{pyridyl}$, 1H). $^{13}C\{^1H\}$ NMR (100.6 MHz, DMSO-d_6): δ 15.6 (CH_3), 15.8 (CH_3), 17.4 (*p*-cym-CH_3,), 21.4 (*p*-cym-CH($\underline{C}H_3$)$_2$), 21.9 (*p*-cym-CH($\underline{C}H_3$)$_2$), 30.4 (*p*-cym-$\underline{C}H(CH_3)_2$), 45.8 (CH_2), 46.2 (CH_2), 52.3 ($(CH_2)_{pyridyl}$), 52.7 ($(CH_2)_{pyridyl}$), 61.4 (d, $^2J_{CP}$ = 12.1 Hz, O-CH_2), 62.4 (O-CH_2), 89.9 (*p*-cym-CH), 90.9 (*p*-cym-CH), 91.2 (*p*-cym-CH), 93.3 (*p*-cym-CH), 102.8 (d, $^3J_{CP}$ = 9.1 Hz, *p*-cym-Cq), 111.76 (*p*-cym-Cq), 121.5 ($(CH)_{BPh4}$), 124.4 ($(CH)_{pyridyl}$), 125.3 ($(CH)_{BPh4}$), 126.0 ($(CH)_{pyridyl}$), 135.5 ($(CH)_{BPh4}$), 139.4 ($(CH)_{pyridyl}$), 158.0 ($(CH=N)_{pyridyl}$), 158.4 ($(CH=N)_{pyridyl}$), 160.4 ($(C=N)_{pyridyl}$), 164.1 (q, J_{CB} = 25.3 Hz, (C-B)$_{BPh4}$). $^{31}P\{^1H\}$ NMR (162 MHz, DMSO-d_6): δ 129.5 (N-P-Ru, 1P), 130.1 (N-P-Ru, 1P). FT-IR (powder, cm^{-1}): *ν*$(CH)_{pyridyl}$ 3055-2983; *ν*(C=N) 1604. HRMS (ESI^+): m/z: 513.0938 $[C_{42}H_{64}Cl_2N_4O_4P_2Ru_2]^{2+}$; HRMS ($ESI^-$): *m/z* 319.1495 BPh_4^-.

Data collection, structure resolution and refinement

Single crystals suitable for X-ray diffraction analysis for compounds **2**, **5a**, **7b** and **8b**, were grown and used to determine the structures for the respective compounds. In a typical experiment, an orange crystal of **7b** with approximate dimensions 0.55 x 0.44 x 0.32 mm^3 was selected under ambient conditions. The crystal was mounted in a stream of cold nitrogen at 150 K and centreed in the X-ray beam using a video camera on the diffractometer. The crystal evaluation and data collection were performed using Quazar multi-layer optics monochromated Mo Kα radiation (λ = 0.71073 Å) on a Bruker D8 Venture kappa geometry diffractometer with duo Iμs sources, a Photon 100 CMOS detector and APEX II control software.[40] All X-ray diffraction measurements were performed at 150(2) K and diffractometer to crystal distance of 4.00 cm. Data reduction was performed using SAINT+, and the intensities were corrected for absorption using SADABS.[42]

Structure resolution and refinement were performed by direct methods using *SHELXT*,[43] and *SHELXL-2014/7*[44] programs. All non-hydrogen atoms were refined with anisotropic displacement coefficients. All hydrogen atoms were placed in geometrically idealised positions and constrained to ride on their parent atoms. Crystallographic data has been deposited with the Cambridge Crystallographic Data Center with CCDC 1843031 (**2**), 1843033 (**5a**), 1843032 (**7b**) and 1843034 (**8b**). Copies of this information may be obtained free of charge from the Director, CCDC, 12 Union Road, Cambridge, CB2 1EZ, UK (fax: +44 1223 336063; deposit@ccdc.cam.ac.uk or http://www.ccdc.cam.ac.uk).

General procedures for the hydrogenation reactions

An autoclave reactor was charged with levulinic acid (10 mmol) catalyst (0.01 mmol / 0.1 mol%), formic acid (10 mmol) and triethylamine (10 mmol). The reactor was purged several times with nitrogen gas and the mixture was stirred at 120 °C for 8 h. After the reaction time had elapsed, the mixture was cooled to room temperature and the gas generated in the course of the reaction was released. A sample of the reaction mixture was taken, diluted with MeOD-d_4 or $CDCl_3$ and analysed by ^1H NMR spectroscopy at 64 scans (5.38 min.).

Acknowledgments

We gratefully acknowledge funding for this project from the National Research Foundation of South Africa (Grant Numbers: 99269 and 117989), The Royal Society and African Academy of Sciences Furture Leaders - African Independent Reseachers (FLAIR) Scheme (Fellowship ref: 191779) and the University of Johannesburg Centre for Synthesis and Catalysis. Our profound gratitude also goes to Prof. Ilia A. Guzei, Dr. Frederick Malan and Dr. Banele Vatsha for their help with the single crystal X-ray data collection.

Keywords: aminophosphinite • phosphoramidite • ruthenium(II) complexes • levulinic acid • γ-valerolactone

[1] Y. Matano, T. Miyajima, N. Ochi, T. Nakabuchi, M. Shiro, Y. Nakao, S. Sakaki and H. Imahori, *J. Am. Chem. Soc.,* **2008**, *130*, 990-1002.

[2] Y. Shaikh, K. Albahily, M. Sutcliffe, V. Fomitcheva, S. Gambarotta, I. Korobkov and R. Duchateau, *Angew. Chem. Int. Ed.,* **2012**, *51,* 1366-1369.

[3] M. C. Copsey and T. Chivers, *Dalton Trans*. **2006**, 4114-4123.

[4] T. Nakajima, Y. Fukushima, M. Tsuji, N. Hamada, B. Kure and T. Tanase, *Organometallics,* **2013**, *32*, 7470-7477.

[5] Y. Ishii, K. Miyashita, K. Kamita and M. Hidai, *J. Am. Chem. Soc.,* **1997**, *119*, 6448-6449.

[6] (a) S. Tanaka, C. Dubs, A. Inagaki and M. Akita, *Organometallics,* **2005**, *24,* 163-184. (b) C. Dubs, T. Yamamoto, A. Inagaki and M. Akita, *Organometallics,* **2006**, *25*, 1344-1358. (c) T. Yamaguchi, T. Koike and M. Akita, *Organometallics,* **2010**, *29*, 6493-6502.

[7] S.-J. Jeon and R. M. Waymouth, *Dalton Trans*., **2008**, 437-439.

[8] (a) C. D. Swor an D. R. Tyler, *Coord. Chem. Rev*., **2011**, *255*, 2860-2881. (b) N. Fey, J. N. Harvey, G. C. Lloyd-Jones, P. Murray, A. G. Orpen, R. Osborne and M. Purdie, *Organometallics,* **2008**, *27*, 1372-1383.

[9] (a) V. Cadierno, P. Crochet, J. Díez, J. García-Álvarez, S. E. García-Garrido and J. Gimeno, *Inorg. Chem.,* **2003**, *42*, 3293-3307. (b) V. Cadierno, P. Crochet, J. Díez, J. García-Álvarez, S. E. García-Garrido, S. García-Grand, J. Gimeno and M. A. Rodríguez, *Dalton Trans*. **2003**, 3240-3249.

[10] T. Nakajima, Y. Kawasaki, B. Kure and T. Tanase, *Eur. J. Inorg. Chem*., **2016**, 4701-4710.

[11] (a) A. Buchard, B. Komly, A. Auffrant, X. F. Le Goff and P. Le Floch, *Organometallics,* **2008**, *27*, 4380-4385. (b) R. B. Siedschlag, V. Bernales, K. D. Vogiatzis, N. Planas, L. J. Clouston, E. Bill, L. Gagliardi and C. C. Lu, *J. Am. Chem. Soc.,* **2015**, *137*, 4638-4641.

[12] A. Buchard, H. Heuclin, A. Auffrant, X. F. Le Goff, and P. Le Floch, *Dalton Trans*., **2009**, 1659-1667.

[13] A. Buchard, E. Payet, A. Auffrant, X. F. Le Goff and P. Le Floch, *New J. Chem*., **2010**, *34*, 2943-2949.

[14] H. Dyer, A. Picot, L. Vendier, A. Auffrant, P. Le Floc and S. Sabo-Etienne, *Organometallics*, **2011**, *30*, 1478-1486.

[15] J.-X. Gao, T. Ikariya and R. Noyori, *Organometallics,* **1996**, *15*, 1087-1089.

[16] M. Gómez, S. Jansat, G. Muller, D. Panyella, P. W. N. M. van Leeuwen, P. C. J. Kamer, K. Goubitz and J. Fraanje, *Organometallics,* **1999**, *18*, 4970-4981.

[17] R. Huber, R. Bigler and A. Mezzetti, *Organometallics,* **2015**, *34*, 3374-3384.

[18] G. Amenuvor, B. C. E. Makhubela, J. Darkwa, *ACS Sustainable Chem. Eng*., **2016**, *4*, 6010-6018.

[19] (a) G. Amenuvor, B. C. E. Makhubela, B. C. E. J. Darkwa, *Catal. Sci. Technol*., **2018**, *8*, 2370-2380. (b) T. Werpy and G. Peterson, U.S Department of Energy NERL/TP-510-35523, 2004, pp. 45-48. (c) I.T. Horváth, *Green Chem*., **2008**, *10*, 1024-1028. (d) V. Fábos, M.Y. Lui, Y.F. Mui, Y.Y. Wong, L.T. Mika, L. Qi, E. Cséfalvay, V. Kovács, T. Szúcs, I.T. Horváth, *ACS Sus. Chem. Eng*., **2015**, *3*, 1899-1904.

[20] (a) A. H. M. de Vries, A. Meetsma and B. L. Feringa, *Angew. Chem.*, **1996**, *108*, 2526-2528. (b) B. L. Feringa, M. Pineschi, L. A. Arnold, R. Imbos and A. H. M. de Vries, *Angew. Chem*., **1997**, *109*, 2733-2736. (c) J. F. Teichert and B. L. Feringa, *Angew. Chem. Int. Ed.*, **2010**, *49*, 2486-2528.

[21] R. N. Firmo, I. C. A. de Souza, F. Miranda, S. da, C. B. Pinheiro, J. A. L. C. Resende and M. Lanznaster, *Polyhedron* **2016**, *117*, 604-611.

[22] S. Oshima, N. Hirayama, K. Kubono, H. Kokusen and T. Honjo, *Analytica Chimica Acta,* **2001**, *441*, 157-164.

[23] A. K. El-Qisairi, H. A. Qaseer, S. F. Alshahateet, M. K. H. Qaseer, M. H. Zaghal, W. Al-Btoush and L. N. Dawe, *Croat. Chem. Acta.,* **2014**, *87*, 123-128.

[24] (a) F. Baig, R. Kant, V. K. Gupta and M. Sarkar, *RSC Adv*. **2015**, *5*, 51220-51232. (b) H. Keypour, M. H. Zebarjadian, M. Rezaeivala, M. Shamsipur, H. R. Bijanzadeh, *J. Solution Chem*., **2014**, *43*, 1218-1231.

[25] D. S. Kissel, J. Florian, C. C. McLauchlan and A.W. Herlinger, *Inorg. Chem.* **2014**, *53*, 3404-3416.

[26] M. S. Balakrishna, R. M. Abhyankar and J. T. Mague, *J. Chem. Soc., Dalton Trans*. **1999**, 1407-1412.

[27] P. Kumar, M. Yadav, A. K. Singh and D. S. Pandey, *Eur. J. Inorg. Chem.* **2010**, 704-715.

[28] H. J. Reich. 5-HMR-8 Symmetry in NMR Spectra: 5-HMR-12 ABX Patterns: https://www.chem.wisc.edu/areas/reich/nmr/05-hmr-12-abx.htm (Accessed on 3rd April 2019).

[29] W. F. Deutsch, M. B. Hursthouse, Z. Kiliç , H. G. Parkes , L. S. Shaw (Née Gözen), R. A. Shaw, *Phosphorus and Sulfur and the Related Element,s* 1987, **32**, 81-85.

[30] L. Deng, J. Li, D.-M. Lai, Y. Fu and Q.-X. Guo, *Angew. Chem. Int. Ed*., **2009**, *48*, 6529-6532.

[31] C. Ortiz-Cervantes, M. Flores-Alamo and J. J. García, *ACS Catal*., **2015**, *5*, 1424-1431.

[32] N. K. Oklu B. C. E. Makhubela, *Inorganica Chim. Acta*, **2018**, *482*, 460-468.

[33] (a) S. Wang, V. Dorcet, T. Roisnel, C. Bruneau and C. Fischmeister. *Organometallics*, **2017**, *36*, 708-713. (b) C. A. M. R. van Slagmaat and S. M. A. De Wildeman, *Eur. J. Inorg.*

Chem., **2018**, 694-702. (c) W. Yang, H. Cheng, B. Zhang, Y. Li, T. Liu, M. Lan, Y. Yu, C. Zhang, W. Lin, S. Fujita, M. Arai and F. Zhao, *Green Chem.*, **2016**, *18*, 3370-3377.

[34] (a) S. Wang, H. Huang, V. Dorcet, T. Roisnel, C. Bruneau and C. Fischmeister, *Organometallics,* **2017**, *36*, 3152-3162. (b) Y. Yi, H. Liu, L.-P. Xiao, B. Wang and G. Song, *ChemSusChem*, **2018**, *11*, 1474-1478.

[35] Z. Lei, Y. Guo, L. Zhao, C. Dai, B. Chen and X. Fang, *Energy Fuels,* **2016**, *30*, 6257-6263.

[36] I. Ayranci, S. Kresta, J. Shen and N. Semagina, *Ind. Eng. Chem. Res.,* **2014**, *53*, 18091-18094.

[37] A. Sharma, C. Julcour, A. A. Kelkar, R. M. Deshpande and H. Delmas, *Ind. Eng. Chem. Res.* **2009**, *48*, 4075-4082.

[38] P. K. Roy, S. Datta, S. Nandi and F. A. Basir, *Fuel,* **2014**, *134*, 39-44.

[39] V. B. Veljkovic, S. H. Lakicevic, O. S. Stamenkovic, Z. B. Todorovic and M. L. Lazic. *Fuel,* **2016**, *85*, 2671-2675.

[40] V. Faḃos, L. T. Mika and I. T. Horvath, *Organometallics,* **2014**, *33*, 181-187.

[41] R. A. Zelonka and M. C. Bair, *Can. J. Chem.* **1972**, *50*, 3063-3072.

[42] APEX2 (including SAINT and SADABS), Bruker AXS Inc., Madison, WI, 2012.

[43] G. M. Sheldrick, *Acta Crystallogr., Sect. A.: Found. Adv.* **2015**, *A71*, 3-8.

[44] G. M. Sheldrick, *Acta Cryst. Sect C: Structural Chemistry* **2015**, *C71*, 3-8.

WILEY-VCH

FULL PAPER

Aminophosphinite and phosphoramidite based Ru^{II} neutral bimetallic complexes form with retention of symmetry. These complexes readily transform into cationic P^N^N^ P complexes following halide abstraction, giving isomers with R,S and S,S configurations. The complexes are good catalysts for levulinic acid hydrogenation into γ-valerolactone

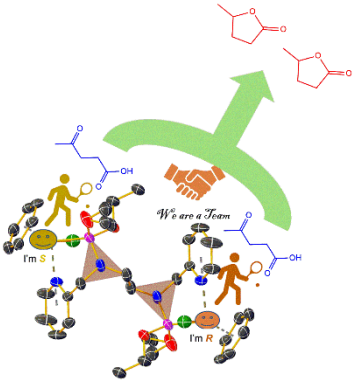

***Phosphorus-based ligands**

Gershon Amenuvor, Charles K. Rono, James Darkwa, and Banothile C. E. Makhubela**

Multidentate pyridyl-aminophosphinite and pyridyl-phosphoramidite ruthenium(II) complexes: Synthesis, structure and application as levulinic acid hydrogenation pre-catalysts.